



## Research paper

# Synthesis, biological evaluation and molecular modeling of 1-oxa-4-thiaspiro- and 1,4-dithiaspiro[4.5]decane derivatives as potent and selective 5-HT<sub>1A</sub> receptor agonists



Silvia Franchini<sup>a</sup>, Leda Ivanova Manasieva<sup>a</sup>, Claudia Sorbi<sup>a</sup>, Umberto M. Battisti<sup>a</sup>, Paola Fossa<sup>b</sup>, Elena Cichero<sup>b</sup>, Nunzio Denora<sup>c</sup>, Rosa Maria Iacobazzi<sup>c,d</sup>, Antonio Cilia<sup>e</sup>, Lorenza Pirona<sup>e</sup>, Simone Ronsisvalle<sup>f</sup>, Giuseppina Aricò<sup>f</sup>, Livio Brasili<sup>a,\*</sup>

<sup>a</sup> Dipartimento di Scienze della Vita, Università degli Studi di Modena e Reggio Emilia, Via Campi 103, 41125, Modena, Italy

<sup>b</sup> Dipartimento di Farmacia, Università degli Studi di Genova, Viale Benedetto XV 3, 16132, Genova, Italy

<sup>c</sup> Dipartimento di Farmacia-Scienze del Farmaco, Università degli Studi di Bari "Aldo Moro", Via E. Orabona 4, I-70125, Bari, Italy

<sup>d</sup> Istituto tumori IRCCS "Giovanni Paolo II", Via Orazio Flacco, 65, 70124, Bari, Italy

<sup>e</sup> Divisione Ricerca e Sviluppo, Recordati S.p.A., Via Civitali 1, 20148, Milano, Italy

<sup>f</sup> Dipartimento di Scienze del Farmaco Sezione di Chimica Farmaceutica e sezione di Farmacologia e Tossicologia, Università degli Studi di Catania, Viale Andrea Doria 6, 95125, Catania, Italy

## ARTICLE INFO

## Article history:

Received 12 June 2016

Received in revised form

15 September 2016

Accepted 16 September 2016

Available online 17 September 2016

## Keywords:

5-HT<sub>1A</sub> receptor

Agonist

Neuroprotection

BBB penetration

Analgesic activity

## ABSTRACT

Recently, 1-(1,4-dioxaspiro[4,5]dec-2-ylmethyl)-4-(2-methoxyphenyl)piperazine (**1**) was reported as a potent 5-HT<sub>1A</sub>R agonist with a moderate 5-HT<sub>1A</sub>R selectivity. In an extension of this work a series of derivatives of **1**, obtained by combining different heterocyclic rings with a more flexible amine chain, was synthesized and tested for binding affinity and activity at 5-HT<sub>1A</sub>R and  $\alpha_1$  adrenoceptors. The results led to the identification of **14** and **15** as novel 5-HT<sub>1A</sub>R partial agonists, the first being outstanding for selectivity (5-HT<sub>1A</sub>/ $\alpha_1$ d = 80), the latter for potency (pD<sub>2</sub> = 9.58) and efficacy (E<sub>max</sub> = 74%). Theoretical studies of ADME properties shows a good profile for the entire series and MDCKII-MDR1 cells permeability data predict a good BBB permeability of compound **15**, which possess a promising neuroprotective activity. Furthermore, in mouse formalin test, compound **15** shows a potent antinociceptive activity suggesting a new strategy for pain control.

© 2016 Elsevier Masson SAS. All rights reserved.

## 1. Introduction

Serotonin (5-hydroxytryptamine, 5-HT) is a relevant neurotransmitter both in the central nervous system and in periphery. It mediates several physiological effects through at least 14 receptor subtypes (5-HT<sub>1-7</sub>: 5-HT<sub>1A-F</sub>, 5-HT<sub>2A-C</sub>, 5-HT<sub>3</sub>, 5-HT<sub>4</sub>, 5-HT<sub>5A</sub>, 5-HT<sub>6</sub>, 5-HT<sub>7</sub>). With the exception of 5-HT<sub>3</sub>, they belong to the seven-transmembrane-spanning receptor or the G-protein-coupled receptor (GPCR) family [1,2]. The 5-HT<sub>1A</sub> receptor (5-HT<sub>1A</sub>R) was the first subtype to be isolated and completely sequenced [3], its pharmacology has been extensively studied and a number of selective ligands have been discovered (Fig. 1). Nowadays this receptor still represents a new attractive target for drug discovery [4].

5-HT<sub>1A</sub>R agonists and partial agonists have been initially employed for the treatment of anxiety, depression, and psychosis [5–9]. Moreover, 5-HT<sub>1A</sub>R agonists have shown neuroprotective properties indicating their utility for the treatment of many neurodegenerative disorders, including Parkinson's disease (PD) and ischemic stroke [10–32]. More recently, it has been shown that 5-HT<sub>1A</sub>R is involved at multiple level in the regulation of nociception and 5-HT<sub>1A</sub>R agonists may represent a new approach in pain relief therapy [33–36].

Among the 5-HT<sub>1A</sub>R ligands, N-1-substituted N-4-arylpiperazines (so-called "long-chain arylpiperazines") have been extensively studied and a generally accepted pharmacophoric model for the recognition of the agonist has been drawn (Fig. 2, panel a) [4,37]. Recently, our research group reported 1-(1,4-dioxaspiro [4,5]dec-2-ylmethyl)-4-(2-methoxyphenyl)piperazine (**1**) as a potent 5-HT<sub>1A</sub>R partial agonist (pD<sub>2</sub> = 8.61) with a moderate selectivity with respect to  $\alpha_1$  adrenoceptors (5-HT<sub>1A</sub>/ $\alpha_1$ a = 18)

\* Corresponding author.

E-mail address: [livio.brasili@unimore.it](mailto:livio.brasili@unimore.it) (L. Brasili).

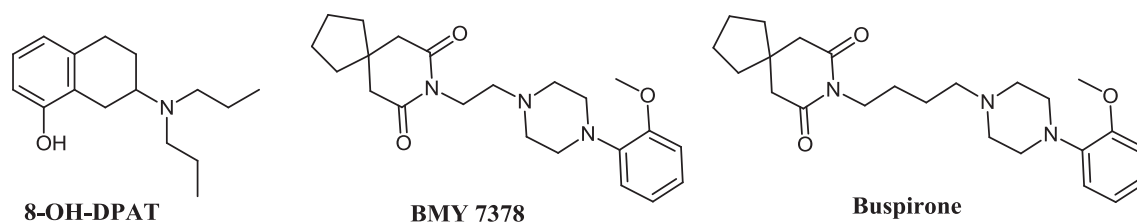


Fig. 1. 5-HT<sub>1A</sub>R selective ligands.

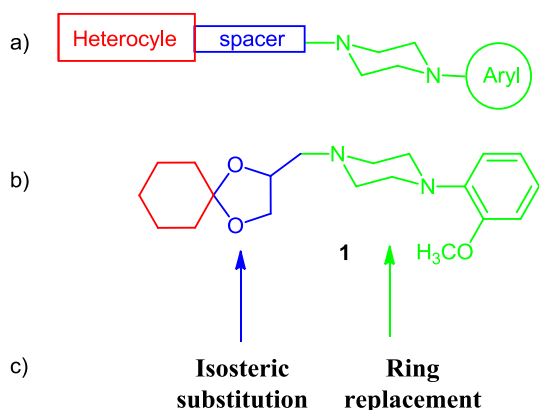


Fig. 2. a) Pharmacophoric model of 5-HT<sub>1A</sub> agonist; b) Chemical structure of compound **1** (pD<sub>2</sub> 5-HT<sub>1A</sub> = 8.61, 5-HT<sub>1A</sub>/α<sub>1</sub> = 18); c) Working hypothesis.

(Fig. 2, panel b) [38]. In a more recent paper, docking of **1** on the newly published 5-HT<sub>1A</sub>R model was performed and a set of structural analogues, substituted at C8 position of the 1,4-dioxaspiro[4.5]decane moiety was explored [39]. All compounds displayed low affinity and activity at 5-HT<sub>1A</sub>R, indicating that only small substituents are allowed, while a higher affinity was observed at α<sub>1</sub>-adrenoceptors, resulting in a significant reversal of selectivity.

With the aim of improving 5-HT<sub>1A</sub>R/α<sub>1</sub> selectivity as well as potency and efficacy, in this work we designed a new set of structural analogues of **1** focusing the attention on both the 1,4-dioxaspiro[4.5]decane and arylpiperazine moieties (Fig. 2, panel c). As regard the first portion, on the basis of previously published data showing that the replacement of one or two ring oxygen atoms with sulfur leads to a progressive decrease of α<sub>1</sub> affinity, the 1-oxa-4-thiaspiro- and 1,4-dithia-spiro[4.5]decane-analogues were synthesized and tested [38]. In addition, the replacement of the piperazine ring with a more flexible basic chain was investigated. By merging these two structural modifications, compound **15** emerged as a potent and selective 5-HT<sub>1A</sub>R agonist endowed with neuroprotective activity *in-vitro* and a potent antinociceptive activity in *in-vivo* model. Finally, molecular modeling on the two GPCRs was performed to better understand the basis of activity and selectivity.

## 2. Results and discussion

### 2.1. Synthesis

The compounds **7–15** were obtained by alkylation of the commercially available 1-(2-methoxyphenyl)piperazine or substituted 2-phenoxyethanamines with the proper chloro- or tosyl-derivative, under microwave irradiation (Scheme 1).

The phenoxyethanamines were easily prepared by reacting the chloroacetamide with the appropriate phenates, followed by reduction of the amides, as previously reported [40]. The 1,3-

dioxolane-, oxathiolane- and dithiolane-scaffolds were readily prepared by acetalization of the cyclohexanone with the proper glycerol derivatives. In the case of 3-mercapto propane-1,2-diol or 2,3-dimercapto propane-1-ol, perchloric acid adsorbed on silica-gel (HClO<sub>4</sub>-SiO<sub>2</sub>) was employed as a new, highly efficient, inexpensive and reusable catalyst for acetal formation, under solvent-free conditions. The hydroxylic group was then converted into a better leaving group (tosylate or chloride) for the subsequent coupling reaction.

### 2.2. Pharmacology

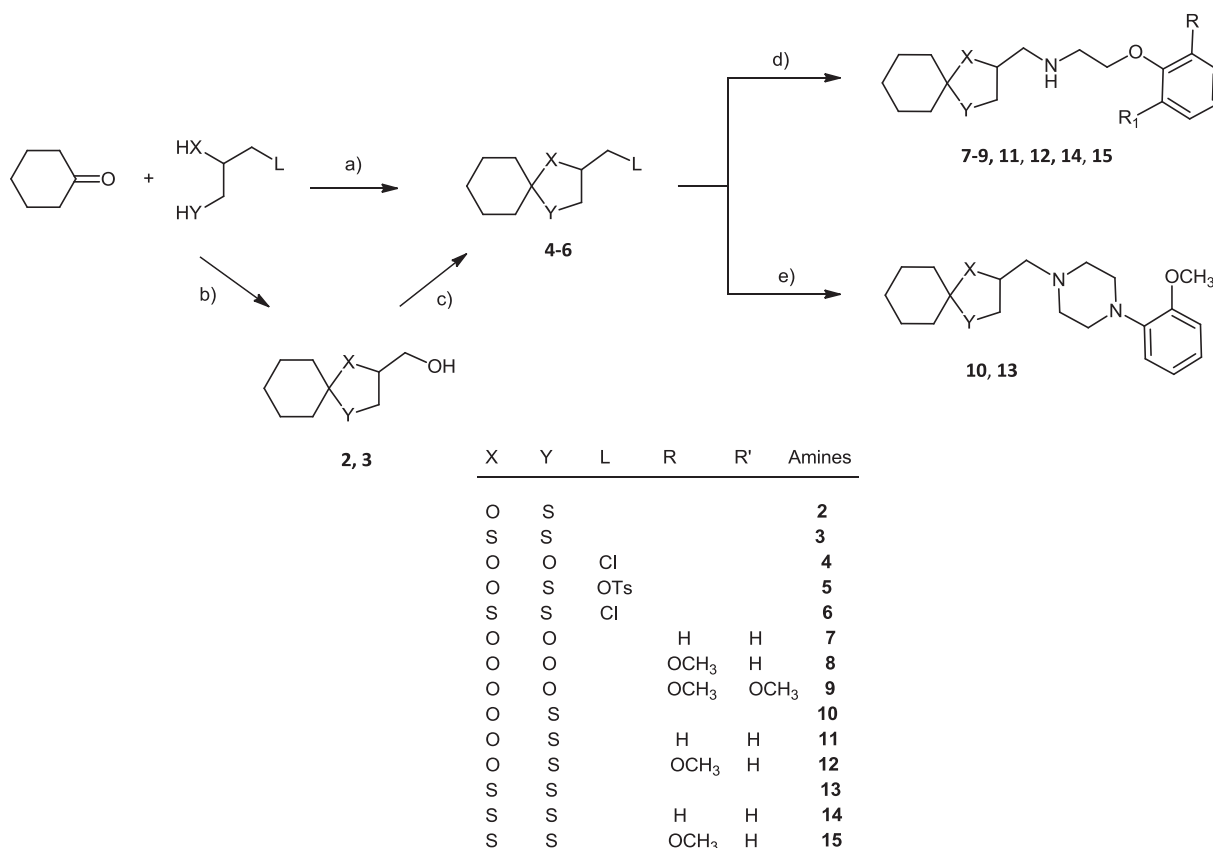
The pharmacological profile of the synthesized compounds **7–15**, the lead compound **1** and BMY-3748, as reference compounds, was evaluated by radioligand binding assays using [<sup>3</sup>H]prazosin to label cloned human α<sub>1</sub> adrenoceptors expressed in CHO cells [41], and [<sup>3</sup>H]8-OH-DPAT to label cloned human 5-HT<sub>1A</sub> receptors expressed in HeLa cells [42].

Functional characterization of the most active and selective compounds (**1**, **13–15**, and BMY-7378) at the 5-HT<sub>1A</sub>R was performed according to methods of Stanton and Beer [43] using [<sup>35</sup>S]GTPγS binding, in cell membranes from HeLa cells transfected with the human cloned 5-HT<sub>1A</sub>R. Stimulation of [<sup>35</sup>S]GTPγS binding was expressed as the percent increase in binding above basal value; maximal stimulation observed with serotonin was established as 100%.

Cytotoxicity assays were carried out against human neuroblastoma cell line SH-SY5Y. Cells were cultured at 37 °C in a humidified incubator containing 5% CO<sub>2</sub> and feed with DMEM (Lonza) nutrient supplemented with 10% heat inactivated FBS, 2 mM L-glutamine, 100 U/mL penicillin and 100 μg/mL streptomycin. Cytotoxicity of compounds is expressed as IC<sub>50</sub> values, the concentrations that cause 50% growth inhibition. The results were determined using the 3-(4,5-dimethylthiazol-2-yl)-2,5-diphenyl-tetrazolium bromide [44].

The neuroprotective capacity of the compounds was tested, as reported by Benckroun et al. [45] Briefly, the ability of the compounds to prevent the human neuroblastoma cell line SH-SY5Y from death was evaluated by using three toxicity models: 1) H<sub>2</sub>O<sub>2</sub>, as a producer of exogenous free radicals, 2) oligomycin A, a mitochondrial respiratory chain blocker which produces mitochondrial ROS by inhibiting the mitochondrial electron-transport chain complex V, and 3) rotenone, showing the same effect of oligomycin A by inhibiting the mitochondrial electron-transport chain complex.

For the assessment of inflammatory pain, mice were subjected to the formalin test. Intraplantar administration of formalin (5%, 10 μl) produces a biphasic nociceptive behavioral response (i.e., licking or biting the injected hind paw). The acute nociceptive phase lasts for the first 10 min, whereas the second inflammatory phase occurs between 15 and 50 min and reflects the development of nociceptive sensitization in the dorsal horns of the spinal cord [46].



**Scheme 1.** Reagents and conditions: a) 3-Chloro-1,2-propanediol, pTsOH, Dean-Stark, 48 h, quantitative for **4**; b) 3-mercapto propane-1,2-diol or 2,3-dimercaptopropan-1-ol, HClO<sub>4</sub>/SiO<sub>2</sub>, r.t., 6 h, 81% for **2**, 71% for **3**; c) TsCl, Et<sub>3</sub>N, DCM, 0 °C to r.t., 12 h, 82% for **5** or SOCl<sub>2</sub>, toluene, 0 °C–80 °C, 12 h, 30% for **6**; d) 2-phenoxyethanamine or (2-methoxyphenoxy)ethanamine or (2,6-dimethoxyphenoxy)ethanamine, KI, 2-methoxyethanol, MW, 160 °C, 30 min, 51% for **7**, 54% for **8**, 54% for **9**, 25% for **11**, 19% for **12**, 15% for **14**, 47% for **15**; e) 1-(2-methoxyphenyl)piperazine, KI, 2-methoxyethanol, MW, 160 °C, 30 min, 67% for **10**, 53% for **13**.

### 2.3. Structure–affinity and structure-activity relationships

All synthesized compounds were tested for binding affinity/activity at 5-HT<sub>1A</sub> and  $\alpha_1$  receptors. Lead compound **1** and BMY-7378 were used as reference compounds on the basis of structure similarities and high affinity/activity for 5-HT<sub>1A</sub>R and  $\alpha_1$  receptors.

As shown in Table 1, the substitution of the 2-methoxy-phenylpiperazine moiety of **1** with the more flexible phenoxyethylamine chains, as for compounds **7–9**, caused substantial changes in binding affinity. In particular, the phenoxy derivative **7** showed a significant decrease in affinity, of about one order of magnitude, for both 5-HT<sub>1A</sub> and  $\alpha_1$  receptors, with the exception for the  $\alpha_{1D}$  subtype, leaving almost unchanged the 5-HT<sub>1A</sub>/ $\alpha_1$  selectivity. The 2-methoxy-phenoxy analogue **8**, showed a 10-fold increased affinity for 5HT<sub>1A</sub>R, compared to **7**, thus restoring the affinity of the lead compound **1** and doubling its 5-HT<sub>1A</sub>/ $\alpha_1$  selectivity, as the increase also seen for  $\alpha_1$  subtypes is to a lesser extent. These results indicate the importance of the 2-methoxy group in stabilizing the binding process (see molecular modeling section). A similar trend was previously observed for the series of the 2,2-diphenyl-1,3-dioxolane derivatives [44]. On the contrary, the introduction of a second methoxy group, as for **9**, caused a drastic loss in affinity at both receptor systems, indicating that a steric hindrance prevents a good anchoring to the binding site.

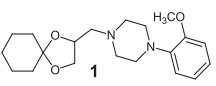
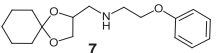
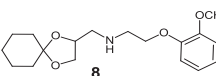
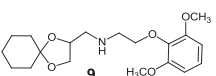
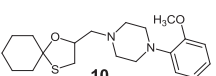
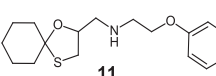
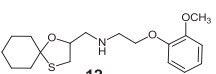
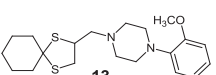
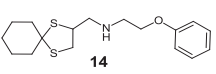
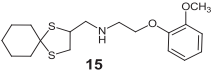
To investigate the effect of the replacement of the ring oxygen atom with a sulfur, 1,3-oxathiolane derivatives **10–12** were prepared. The binding data showed that at 5HT<sub>1A</sub>R this substitution leaves unchanged the affinity, while it produces some effect on  $\alpha_1$

adrenoceptors. A significant increases of affinity was observed only for  $\alpha_{1D}$  subtype in the 1,3-oxathiolane series (**10–12**) compared to the corresponding 1,3-dioxolanes (**1**, **7**, **8**), thus the 5-HT<sub>1A</sub>/ $\alpha_1$  selectivity ratio is halved. Again, the 2-methoxyphenoxy derivative **12** showed the highest 5-HT<sub>1A</sub> affinity within this series (**12** > **10** >> **11**).

Surprisingly, when both oxygen atoms are replaced by sulfur, as for the 1,3-dithiolane derivatives **13–15**, the affinity at 5-HT<sub>1A</sub>R increased, while, at  $\alpha_1$  subtypes, it is decreased or unchanged. The enhancement at 5-HT<sub>1A</sub>R is remarkable only for **14**, whose affinity is 15- and 24-fold higher than the ones of the corresponding 1,3-oxathiolane **11** and 1,3-dioxolane **7**. In this case the role of the 2-methoxy group on the phenoxyethylamine chain is less relevant, as the variations in affinity, especially at 5-HT<sub>1A</sub>R, is very limited and scarcely significant. This is probably due to an additional interactions of the 1,4-dithia-spiro[4.5]-decane moiety of **14** in stabilizing the binding mode of the protein-ligand complex, by several contacts with a deep receptor cavity, including V117, K191, Y195, T196, S199, T200, F361, F362, A365 (see molecular modeling section). Among all, **14** is outstanding in terms of selectivity with a 5-HT<sub>1A</sub>/ $\alpha_1$  ratio of 80. These findings support the previously published data and seem to confirm that moving from 1,3-dioxolanes or 1,3-oxathiolanes to 1,3-dithiolanes the affinity and/or selectivity at/for 5-HT<sub>1A</sub>R progressively increases [44]. With the exception of compounds **7** and **11**, the same improvement is observed by replacing the 2-methoxyphenylpiperazine with the more flexible 2-methoxy-phenoxyethylamine.

Functional characterization at 5-HT<sub>1A</sub>R was performed for the

**Table 1**  
Affinity constants (pK<sub>i</sub>)<sup>a</sup> and selectivities<sup>b,c</sup> of test and reference compounds for the human recombinant  $\alpha_1$  adrenoceptor subtypes and the 5-HT<sub>1A</sub>R.

Compound	$\alpha_{1a}$ <sup>a</sup>	$\alpha_{1b}$ <sup>a</sup>	$\alpha_{1d}$ <sup>a</sup>	5-HT <sub>1A</sub> <sup>a</sup>	$\alpha_{1d}/\alpha_{1a}$ <sup>b</sup>	$\alpha_{1d}/\alpha_{1b}$ <sup>b</sup>	$\alpha_{1b}/\alpha_{1a}$ <sup>b</sup>	5-HT <sub>1A</sub> / $\alpha_1$ <sup>c</sup>
 <b>1</b>	7.04	6.90	<6	8.29	<0.1	<0.1	0.7	18
 <b>7</b>	<6	6.01	6.26	7.43	1.8	1.7	1	15
 <b>8</b>	6.64	6.41	7.02	8.52	2.4	4	0.6	31
 <b>9</b>	<6	<6	5.75	<6	0.5	0.5	1	1
 <b>10</b>	7.24	6.72	7.41	8.30	1.5	4.9	0.3	7.8
 <b>11</b>	<6	6.36	6.67	7.64	4.7	2	2.3	9.3
 <b>12</b>	6.57	6.66	7.49	8.65	8.3	6.8	1.2	14.4
 <b>13</b>	6.70	6.39	7.00	8.52	2	4	0.5	33
 <b>14</b>	<6	6.26	6.91	8.81	8	4.5	1.8	79
 <b>15</b>	6.73	6.71	7.46	9.03	5.4	5.6	1	37
BMY-7378	6.41	6.15	8.89	8.90	295	550	2	1

<sup>a</sup> K<sub>i</sub> values were derived from the Cheng–Prusoff equation [47] at one or two concentrations and agreed within 10%.

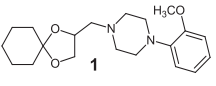
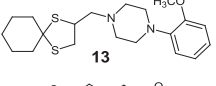
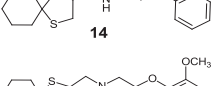
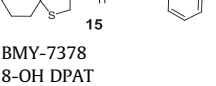
<sup>b</sup> Antilog of the difference between the pK<sub>i</sub> values for  $\alpha_{1a}$ ,  $\alpha_{1b}$  and  $\alpha_{1d}$  adrenoceptors.

<sup>c</sup> Antilog of the difference between the pK<sub>i</sub> values for 5-HT<sub>1A</sub>R and  $\alpha_1$  adrenoceptors (higher value).

most promising compounds (**13–15**). The results are reported in Table 2. In stimulation experiments, compounds **13–15** increased the binding of [<sup>35</sup>S]GTPγS with pD<sub>2</sub> values of 8.61, 8.27 and 9.58, respectively. The E<sub>max</sub> values were of 37, 85 and 74, defining the three compounds as partial agonists. Notably, the most active

compound **15** exhibited an improved potency (10-fold) and efficacy (1.5 fold) compared to the lead compound **1**, with a pD<sub>2</sub> value higher (10-fold) than that of the reference full agonist 8-OH-DPAT (pD<sub>2</sub> = 8.49, Fig. 3).

**Table 2**  
Agonist potency (pD<sub>2</sub>), relative effectiveness (E<sub>max</sub>) in the agonist-induced [<sup>35</sup>S]GTPγS-binding assay at the human 5-HT<sub>1A</sub> receptor.

Compound	pD <sub>2</sub>	E <sub>max</sub> <sup>a</sup>
 <b>1</b>	8.61	48
 <b>13</b>	8.61	37
 <b>14</b>	8.27	85
 <b>15</b>	9.58	74
BMY-7378	9.27	26
8-OH DPAT	8.49	100

<sup>a</sup> Maximal stimulation expressed as a percentage of the maximal 5-HT response.

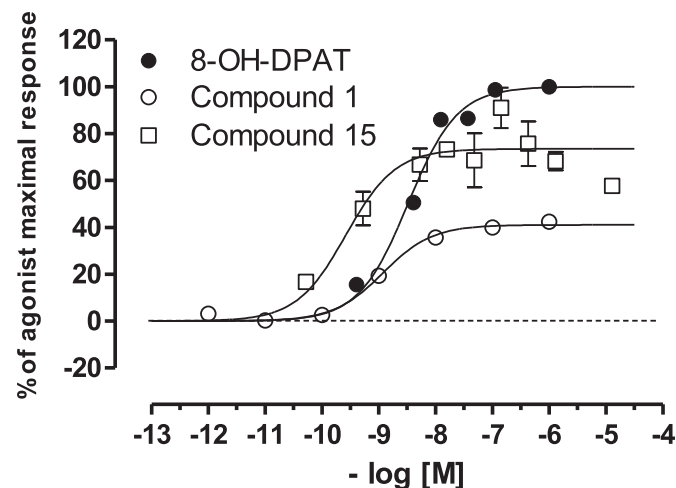


**Fig. 3.** Stimulation of [<sup>35</sup>S]GTPγS binding in HeLa cells expressing human recombinant 5-HT<sub>1A</sub>R by compound **15** and the reference full agonist 8-OH-DPAT.

## 2.4. Prediction of ADMET properties

The computational prediction of descriptors related to absorption, distribution, metabolism, excretion and toxicity properties (ADMET) represents a useful *in silico* strategy accelerating the lead compound discovery process [48].

In this work, for compounds **1**, **7–15** extent of blood-brain barrier permeation (LogBBB), rate of passive diffusion-permeability (LogPS), human intestinal absorption (HIA), volume of distribution (Vd), median lethal dose (LD<sub>50</sub>) related to oral administration and the logarithmic ratio of the octanol-water partitioning coefficient (cLogP) were calculated.

As shown in Table 5, all the compounds are characterized by a favourable profile in terms of lipophilicity, being the calculated LogP below 5 (Lipinski rules) and also display the ability to fully be adsorbed at the human intestinal membrane. Notably, compounds **1**, **10**, **13–15** show higher blood-brain barrier permeation with respect to the other compounds, being in any case all of them able to pass at the central nervous system. Finally, all the compounds exhibit a favourable toxicity profile, being the estimated LD<sub>50</sub> in the range of 600–1200 mg/kg for mouse after oral administration.

## 2.5. Neuroprotective capacity of compound 15

The neuroprotective capacity of **15** was tested for its ability to prevent the human neuroblastoma cell line SH-SY5Y from cell death induced by three toxicity models: 1) hydrogen peroxide for the generation of exogenous free radicals, 2) oligomycin A, a mitochondrial respiratory chain blocker which produces mitochondrial ROS by inhibiting the mitochondrial electron-transport chain complex V, and 3) rotenone, showing the same effect of oligomycin A by inhibiting the mitochondrial electron-transport chain complex I [45]. Before the assessment of the neuroprotective capacity, the direct cytotoxicity of compound **15** was investigated and cell viability after 24 h of exposure was measured by MTT assay across a wide concentration range (0.1–100 μM). The IC<sub>50</sub> values were 195 ± 1.7, 29 ± 3.4, 74.1 ± 4.5 and 51 ± 5 μM for H<sub>2</sub>O<sub>2</sub>, oligomycin A, rotenone and compound **15**, respectively. Therefore, in the neuroprotective test, compound **15** was used at a concentration of 0.1 and 1 μM. In particular, as reported in Table 3, compound **15** showed good neuroprotective effect against the insult caused by oligomycin A and H<sub>2</sub>O<sub>2</sub> (only at concentration of 0.1 μM) whereas it exhibited a minimum neuroprotection against rotenone, at the two tested concentrations.

**Table 3**  
Calculated ADMET properties for compounds **1**, **7–15**.

Comp.	LogBBB <sup>a</sup>	LogPS <sup>b</sup>	HIA (%) <sup>c</sup>	Vd (l/kg) <sup>d</sup>	LD <sub>50</sub> (mg/kg) <sup>e</sup>	cLogP
<b>1</b>	0.76	−1.2	100	4.1	640	3.24
<b>7</b>	0.26	−1.6	100	3.3	1200	2.88
<b>8</b>	0.21	−1.9	100	3	1200	2.52
<b>9</b>	0.26	−1.9	100	2.8	1200	2.83
<b>10</b>	0.82	−1.1	100	3.5	680	3.96
<b>11</b>	0.42	−1.3	100	6	1100	3.80
<b>12</b>	0.32	−1.6	100	5.6	1000	3.30
<b>13</b>	0.89	−1.1	100	3.4	600	4.58
<b>14</b>	0.75	−1.2	100	6.2	890	4.49
<b>15</b>	0.61	−1.3	100	5.7	870	4.15

<sup>a</sup> Extent of brain penetration based on ratio of total drug concentrations in tissue and plasma at steady-state conditions.

<sup>b</sup> Rate of brain penetration. PS represents Permeability-Surface area product and is derived from the kinetic equation of capillary transport.

<sup>c</sup> HIA represents the human intestinal absorption, expressed as percentage of the molecule able to pass through the intestinal membrane.

<sup>d</sup> Prediction of Volume of Distribution (Vd) of the compound in the body.

<sup>e</sup> Acute toxicity (LD<sub>50</sub>) for mouse after oral administration (RI ≥ 30).

## 2.6. Bi-directional transport studies on MDCKII-MDR1 monolayers

Many cell-based *in-vitro* methods have been developed to determine the BBB permeation of compounds under investigation. Among them, MDCK-MDR1 cell line represents a well-established *in-vitro* method mimicking the BBB [49–51]. It is well known that MDCKII-MDR1 cells form tight monolayers and express P-glycoprotein (P-gp), which is specifically involved in the efflux transport of drugs from the BBB. In particular, we were interested in assessing whether compound **15** is able to permeate MDCK-MDR1 monolayers and to interact with P-gp. Thus, transport studies were conducted both in AP-to-BL and BL-to-AP direction and the results are reported in Table 4. Compound **15** showed not significant differences in  $P_{app}$  values between AP-to-BL and BL-to-AP direction and the efflux ratio (ER) calculated by the equation  $ER = P_{app, BL-AP}/P_{app, AP-BL}$  was found to be less than 2, indicating that this compound is not likely to be considered substrate for P-gp transport. These results suggest that **15** is able to permeate the monolayer by passive diffusion with permeability values comparable to diazepam. The results for the controls were within the expected values.

## 2.7. Antinociceptive activity

Compound **15**, endowed with high affinity and high agonist potency, was chosen for determining potential analgesic activity *in-vivo*. For the assessment of which, mice were subjected to the formalin test. As shown in Fig. 4, compound **15** was administered 15 min before formalin at the dose of 3, 5 and 10 mg/kg i.p. The dose of 10 mg/kg was able to induce a significant analgesic effect in the second phase of formalin test (\* $p < 0.05$ ). Pretreatment with the selective 5-HT<sub>1A</sub>R antagonist WAY-100635 (3 mg/kg i.p.), 30 min before of compound **15** (10 mg/kg i.p.), prevented its analgesic effect (# $p < 0.05$ ). WAY-100635 (3 mg/kg i.p.), *per se* at least at the used dose, did not modify the licking response after formalin injection (Fig. 5).

## 2.8. Molecular modeling

Molecular modeling studies have been undertaken in order to better elucidate the affinity and selectivity profiles of the newly synthesized analogues of compound **1**. To gain a perspective of the most relevant patterns of key contacts involved in the ligand binding mode, we performed our work based on 5-HT<sub>1A</sub>R and  $\alpha_{1D}$ R homology models. In the first case, we relied on the previously built 5-HT<sub>1A</sub>R theoretical model employed in docking studies of several *in-house* series of 5-HT<sub>1A</sub> ligands [39,52,53].

For the human  $\alpha_{1D}$  receptor, a specific model has been built and is here discussed, focusing our attention on  $\alpha_{1D}$ R subtype, because of the high affinity values shown by all compounds.

## 2.9. $\alpha_{1D}$ homology modeling

The 3D structure of the human  $\alpha_{1D}$  receptor has been generated following the ligand-based homology modeling strategy proposed by Moro [54]. This computational option is very useful to build a

**Table 4**  
Protective effect of compound **15** on SH-SY5Y cell death induced by H<sub>2</sub>O<sub>2</sub> or oligomycin A or rotenone. Data are expressed as percent neuroprotection ± SD of three independent experiments.

Compd [μM]	H <sub>2</sub> O <sub>2</sub> (195 μM)	Oligomycin A (30 μM)	Rotenone (75 μM)
<b>15</b> (1 μM)	66 ± 4	86 ± 5	66 ± 2
<b>15</b> (0.1 μM)	83 ± 6	81 ± 4	62 ± 2

**Table 5**  
Bi-directional Transport Across MDCKII-MDR1 cells of compound **15**.

Compd	$P_{app}$ AP (cm/sec)	$P_{app}$ BL (cm/sec)	ER <sup>a</sup> $P_{app}BL/P_{app}AP$
<b>15</b>	$1.11 \times 10^{-5}$	$1.09 \times 10^{-5}$	0.98
Diazepam	$1.46 \times 10^{-5}$	$1.23 \times 10^{-5}$	0.84
FD-4	$1.03 \times 10^{-6}$	$2.08 \times 10^{-7}$	0.20

<sup>a</sup> Efflux ratio (ER) was calculated using the following equation:  $ER = P_{app, BL-AP} / P_{app, AP-BL}$ , where  $P_{app, BL-AP}$  is the apparent permeability of basal-to-apical transport, and  $P_{app, AP-BL}$  is the apparent permeability of apical-to-basal transport. An efflux ratio greater than 2 indicates that a test compound is likely to be a substrate for P-gp transport.

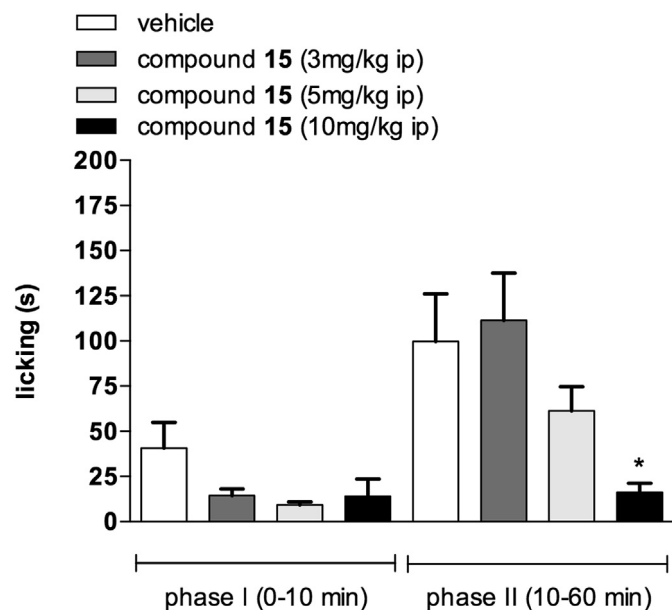


**Fig. 4.** Effect of intraperitoneal (i.p.) injection of **15** (3, 5 or 10 mg/kg) on the first (0–10 min) and second (10–60 min) phase of the formalin test. Test compound or vehicle were injected 15 min prior to the intraplantar injection of formalin. Data are means + S.E.M. of 8–10 mice per group. \* $p < 0.05$  vs. the respective groups of mice injected with vehicle.

homology model in the presence of a ligand docked into the primary template and has been widely and fruitfully used to build GPCR so as enzyme models [55–57]. In this case we selected a structurally-related analogue of compound **1** (compound **A**, as shown in Fig. 6), exhibiting high degree of affinity and selectivity toward the  $\alpha_{1D}$  receptor ( $pK_i \alpha_{1D} = 9.09$ ,  $\alpha_{1D}/5-HT_{1A} = 28$ ) [38].

Accordingly, **A** was docked into the  $\beta_2$ -adrenoreceptor X-ray coordinates (pdb: 2RH1) and employed in the building and refinement of the derived  $\alpha_{1D}$  model. This kind of approach allowed us to set up a much more suitable receptor model, to be used for efficiently exploring the putative binding mode of analogues **7–15**. The sequence alignment of the  $\alpha_{1D}$  receptor (P25100) with respect to the human  $\beta_2$ -adrenoreceptor (pdb: 2RH1) coordinates is shown in Fig. 7. The reliability of the alignment was verified by the high value of the pairwise percentage residue identity (PPRI = 42%). Accordingly, a consistent number of  $\alpha_{1D}$  residues resulted to be conserved in comparison with those of the  $\beta_2$ -adrenoreceptor TM helices: (i) V97, G98, L108, V111, G113, N114, L116, V117, I118, A122 in TM1, (ii) V130, T131, N132, Y133, F134, I135, L138, A139, A141, D142, L143, V149, P151, F152, A154 in TM2, (iii) G165, C168, W172, D176, V177, L178, C179, T181, A182, S183, F184, L187, C188, I190, V192, D193, R194, Y195 in TM3 (the DRY motif; 193–195 residues), (iv) K212, A213, I216, W221, V223,

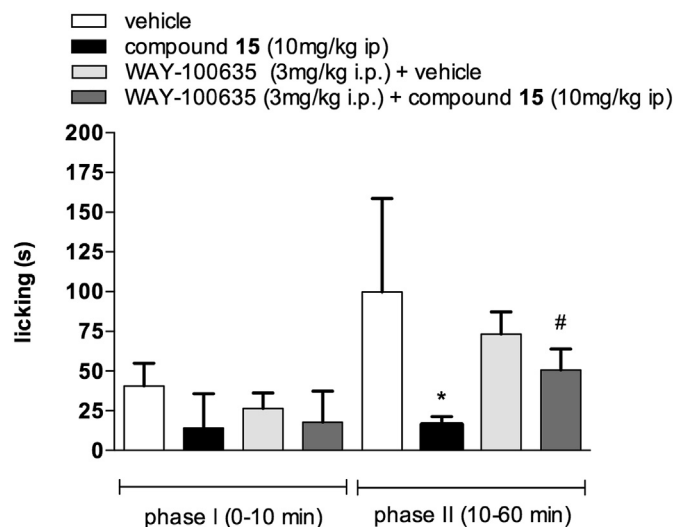


**Fig. 5.** Effect of WAY-100635 (3 mg/kg i.p.) on analgesia induced by **15** (10 mg/kg i.p.) during the first (0–10 min) and second (10–60 min) phase of the formalin test. Test compound or vehicle were injected 15 min prior to the intraplantar injection of formalin. WAY-100635 was injected 30 min prior to **15** or vehicle. Data are means + S.E.M. of 8–10 mice per group. \* $p < 0.05$  vs. the respective groups of mice injected with vehicle. # $p < 0.05$  vs mice treated with **15** (10 mg/kg i.p.).

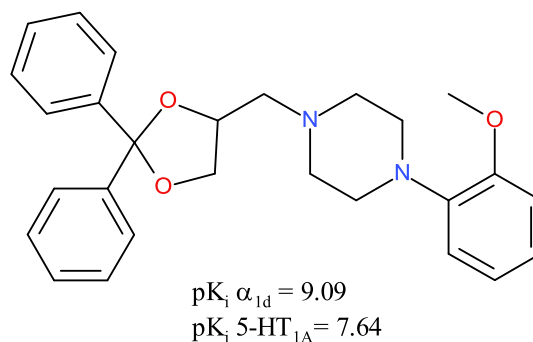


**Fig. 6.** Structure of compound **A**.

S228 P231 in TM4, (v) Y254, A255, S258, S259, S262, F263, Y264, P226, V269, I270, V272, Y274, R276, V277 in TM5, (vi) E343, K345, A346, K348, T349, L350, I352, G355, F357, L359, C360, W361, P363, F364, F365, V367 in TM6 (CWXP motif; 360–363 residues); (vii) E381, V383, W389, G391, Y392, N394, S395, N398, P399, L400, I401, Y402, C404 in TM7 (NPXIY motif; 398–402 residues).

The derived backbone conformation was inspected by Ramachandran plot (showing absence of outliers) and superimposed to the coordinates of the template structure (RMSD = 0.747 Å; Fig. 8). See Materials and Methods Section for further computational details.

### 2.10. Molecular docking of compound **A**

In a second computational step, ligand **A** was docked into the two in-house GPCRs models in order to examine and compare the corresponding binding modes at the  $\alpha_{1D}$  and 5-HT<sub>1A</sub> receptors. According to our calculation, **A** (the *R* enantiomer proved to be the most probable) was highly stabilized into the  $\alpha_{1D}$  binding site through a salt-bridge interaction between the piperazine protonated nitrogen atom and the conserved D176, and by two H-bonds between: (i) one oxygen atom of the 1,3-dioxolane core and Y254 side-chain; (ii) the methoxy group and K385  $\epsilon$ -amino group.

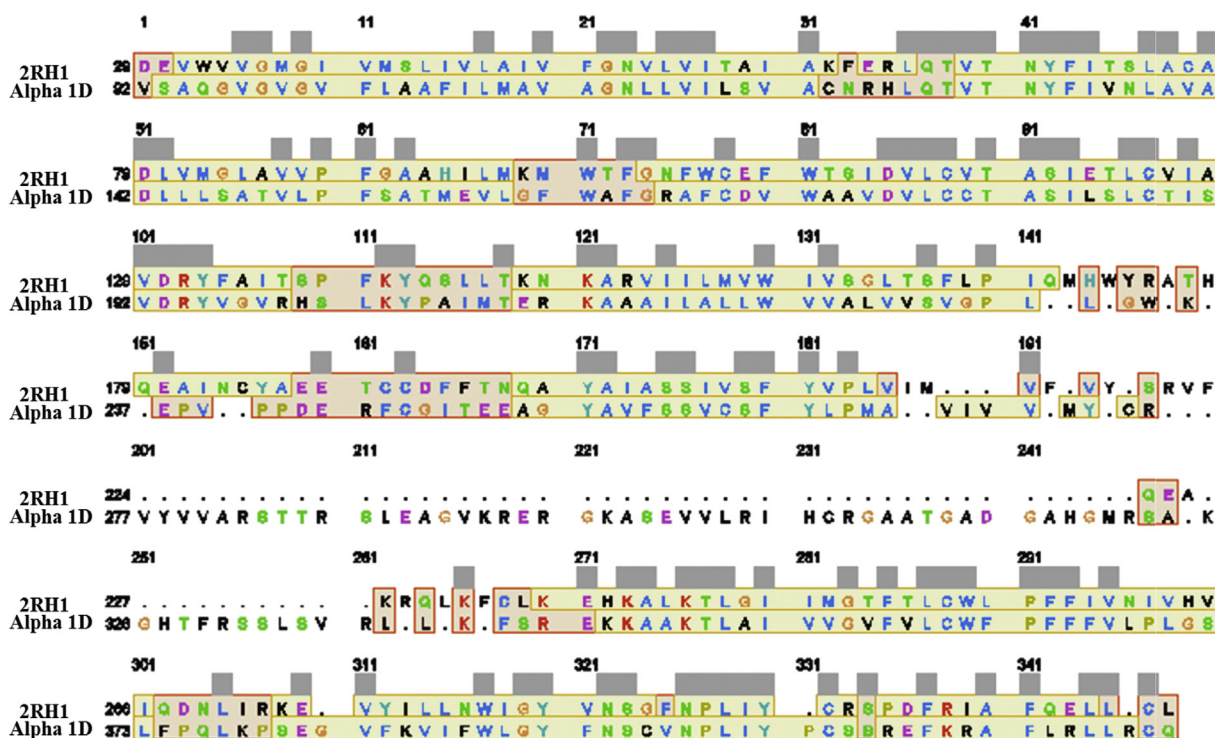


Fig. 7. Sequence alignment of the  $\alpha_{1D}$  on the human  $\beta_2$ -adrenoreceptor (pdb: 2RH1) coordinates. Any conserved region is displayed by grey histograms. All the residues included in  $\alpha$ -helix and loop domains are highlighted in light yellow and pink, respectively. (For interpretation of the references to colour in this figure legend, the reader is referred to the web version of this article.)

Furthermore, the 2-methoxyphenyl ring and the diphenyl substituents were also engaged in  $\pi$ - $\pi$  stacking with W172, F388 and Y254, F364 and F365, respectively (Fig. 9).

Differently, at 5HT<sub>1A</sub>R, ligand **A** (the *R* enantiomer proved to be the most probable;  $pK_i$  5-HT<sub>1A</sub> = 7.64) displayed a salt-bridge between the piperazine protonated nitrogen atom and the key residue D116, while only one H-bond was detected between the oxygen atom of the dioxolane ring and Y390. The lack of an additional H-bond interaction of the methoxy group into the 5HT<sub>1A</sub> binding site turned around the docking pose of **A** with respect to  $\alpha_{1D}$  adrenoreceptor. In this case, the methoxyphenyl ring and the diphenyl portion were oriented towards Y195, F362 and Y96, F112, Y390 respectively, determining  $\pi$ - $\pi$  stacking interactions (Fig. 10).

However, this orientation was detrimental for the binding with the 5-HT<sub>1A</sub>R, as confirmed by the biological data showing a lower affinity at 5-HT<sub>1A</sub> ( $pK_i$  = 7.64) with respect to  $\alpha_{1D}$  ( $pK_i$  = 9.09) (Fig. 6).

Notably, these results highlighted a number of amino acids interacting with the ligands which are conserved within 5-HT<sub>1A</sub>R and  $\alpha_{1D}$ , in particular a key aspartic acid residue, showing that the two protein binding sites share a quite common hydrophobic/hydrophilic trend. In particular, the amino acids contributing to the ligand binding were classified by us into two sets:

- a first set consisting of specific residues present in both receptors and implicated in strong interactions. For example the acidic D176 in  $\alpha_{1D}$ R or D116 in 5-HT<sub>1A</sub>R, which represent the common anchoring point through the formation of a salt-bridge interaction plus some polar residues like Y254 for  $\alpha_{1D}$ R and Y195 for 5-HT<sub>1A</sub>R, which further stabilize the ligand binding through an H-bond interaction;
- a second set referring to specific amino acids present only in 5-HT<sub>1A</sub>R or  $\alpha_{1D}$ R, allowing the formation of H-bonds responsible of the ligand specificity towards the receptor. For example K385 in

$\alpha_{1D}$ R and N386 in 5-HT<sub>1A</sub>R seem to be fundamental in conferring specificity. Thus, any focused H-bond with K385 or N386 residue, might allow the discovery of more selective ligands towards  $\alpha_{1D}$  or 5-HT<sub>1A</sub>R, respectively.

### 2.11. 5-HT<sub>1A</sub>R docking-studies

In our previous works we deeply investigated through docking studies 1,3-dioxolane-, 1,3-oxathiolane-, 1,3-dithiolane-, spiro-dioxolane-tetrahydrofuran-, cyclopentanone- and cyclopentanol-based derivatives as 5-HT<sub>1A</sub> ligands, whose affinity profile proved to be due to the presence of a proper basic feature interacting with the aspartic acid D116. Moreover, agonists and antagonists could also exhibit additional contacts with N386 and Y390, and with K191, respectively [52,53].

Notably, a number of following docking studies reported in literature described a unique receptor cavity involved in the 5-HT<sub>1A</sub> full agonists, partial agonists and antagonists binding [58–60], giving a further validation to our previous computational findings. Indeed, H-bond interactions between agonists and D116 and N386 were reported in literature, falling in a crevice delimited by F112, I113, D116, K191, while partial agonists as well as antagonists were H-bonded at least with D116.

Docking studies on compounds **7–15** here performed within the previously built 5-HT<sub>1A</sub>R homology model [39,52,53] allowed us to further explore their structure-activity relationships (SAR) and to gain more insight about the pattern of substitutions involved in their affinity. According to our calculations, the 1,4-dioxaspirodecane derivatives **7** and **8** shared the same docking mode of the previously described compound **1** [39]. Indeed, both compounds (the *R* enantiomers proved to be the most probable;  $pK_i$  5-HT<sub>1A</sub> = 7.43, 8.53), were properly stabilized into the 5-HT<sub>1A</sub> binding site through the key salt-bridge between the protonated

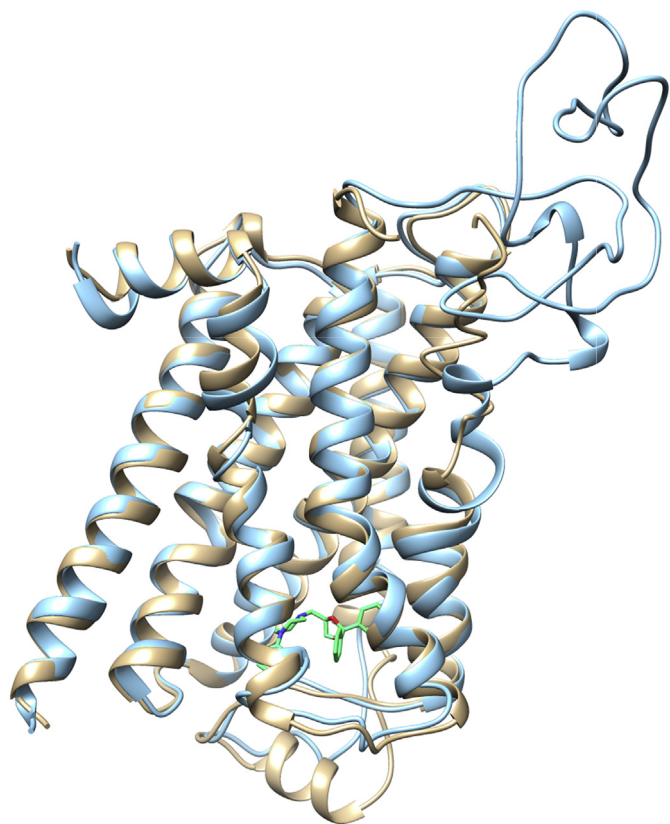


**Fig. 8.** The superimposition of the final  $\alpha_{1D}$  model (backbone in cyan) on the human  $\beta_2$ -adrenoreceptor 2RH1 coordinates (backbone in khaki) is depicted. Ligand **A** structure is also depicted in stick (C atom: light green). (For interpretation of the references to colour in this figure legend, the reader is referred to the web version of this article.)

nitrogen atom and D116. Moreover, one H-bond interaction between the secondary amine and Y390 side chain was detected, as for **1**, while the 1,4-dioxaspirodecane moiety occupied a

hydrophobic cavity delimited by A93, Y96, Q97, F112, A383, I384 and Y390. Notably, unlike **1**, compound **8** was able to establish an additional H-bond between the 2-methoxy oxygen atom and Y195 (Fig. 11).

This kind of positioning could be due to the presence of a flexible linker, as observed within all the members of the series (dioxo-, oxathia-dithiaspiro-decane derivatives), being in agreement with the higher affinity values of **8**, **12** and **15** with respect to **1**, **10** and **13**. Conversely, compound **9**, bearing a slightly bulkier amine chain, was unable to occupy the ligand binding site.

Interestingly, the members of the oxathia- (**10**, and **11**, **12** the *S* and the *R* enantiomers proved to be the most probable) and dithiaspiro-decane series (**13**, and **14**, **15** the *S* and the *R* enantiomers proved to be the most probable) displayed a switched ligand binding mode, maintaining in any case a salt-bridge with D116, while the methoxy-analogues (**10**, **12** and **13**, **15**) also exhibited H-bonds with Y390 (in Fig. 12 the docking mode of **12** and **15**, taken as reference compounds for the two series, are depicted).

The replacement of the dioxaspiro-decane of the prototype **1** with the much more bulkier oxathia- and dithiaspiro-decane moved the ligand cyclohexyl ring towards a deeper cavity including residues V117, K191, Y195, T196, S199, T200, W358, F362, A365, partially constraining the phenoxyethylamine chain flexibility. Consequentially, the dithiaspiro decane derivatives **14** and **15** resulted highly stabilized into the 5-HT<sub>1A</sub>R binding site also by H-bonds with N386, which proved to be a key residue for 5-HT<sub>1A</sub>R agonism and selectivity. Accordingly, among all the compounds studied in this work, **14** and **15** showed the highest 5HT<sub>1A</sub>/ $\alpha_{1D}$  selectivity ratio (79 and 37, respectively).

## 2.12. $\alpha_{1DR}$ docking-studies

In order to rationalize the low affinity values observed at  $\alpha_{1DR}$ , the compounds were docked into the corresponding homology model. Briefly, all the ligands displayed a salt-bridge interaction between the protonated nitrogen atom and D176 anchoring residue. Moreover, when a methoxy group is present, as for compounds **8**, **10**, **12**, **13** and **15**, an H-bond interaction with Y254 side-

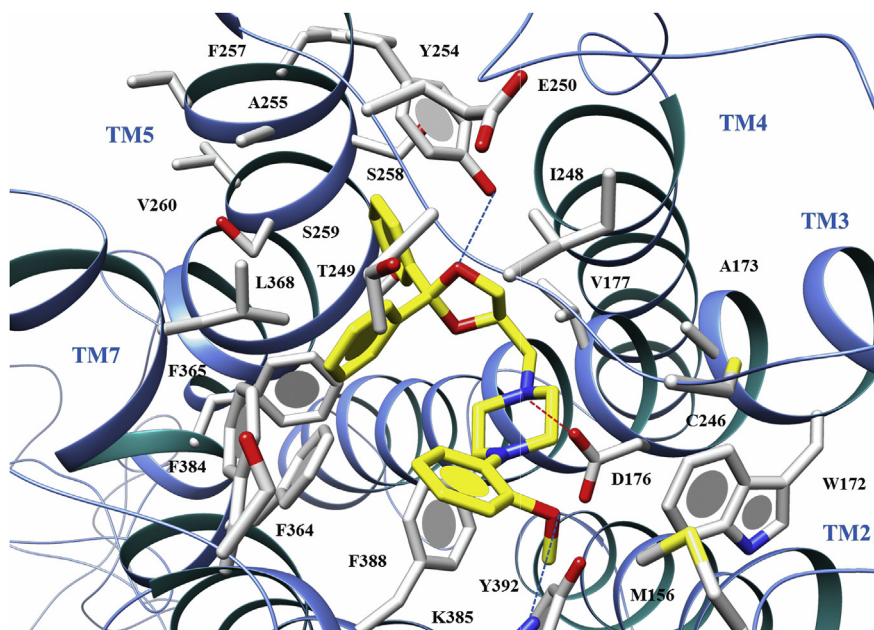


**Fig. 9.** The ligand **A** docking pose into the final  $\alpha_{1D}$  binding site is reported. The ligand is coloured by atom-type (C atom: yellow). Salt-bridge and H-bond contacts are displayed by line and coloured in red and light blue, respectively. (For interpretation of the references to colour in this figure legend, the reader is referred to the web version of this article.)



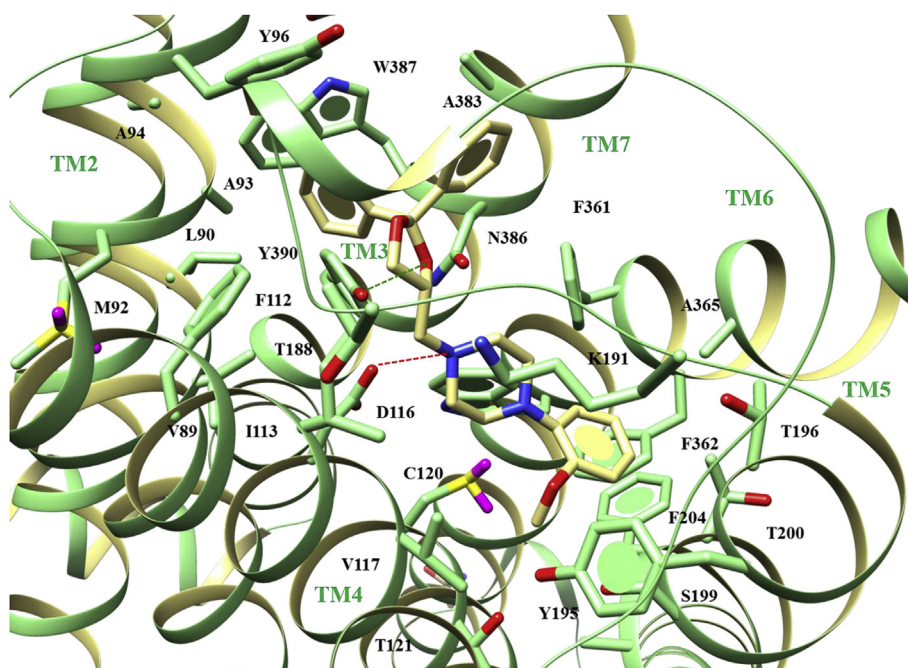


**Fig. 10.** The ligand **A** docking pose into the 5HT<sub>1A</sub> binding site is reported. The ligand is coloured by atom-type (C atom: khaki). Salt-bridge and H-bond contacts are displayed by line and coloured in red and light green, respectively. (For interpretation of the references to colour in this figure legend, the reader is referred to the web version of this article.)

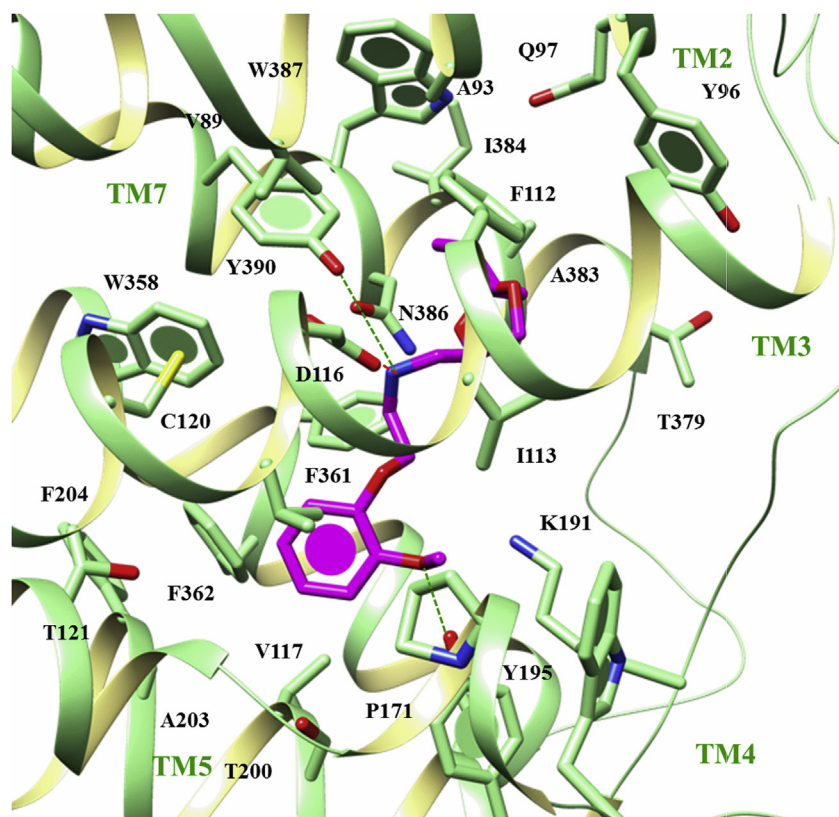


**Fig. 11.** The **8** docking pose into the 5HT<sub>1A</sub> binding site is reported. The ligand is coloured by atom-type (C atom: magenta). Salt-bridge and H-bond contacts are displayed by line and coloured in red and light green, respectively. (For interpretation of the references to colour in this figure legend, the reader is referred to the web version of this article.)

chain is detected (in Fig. 13 the docking mode of **12** and **15** are depicted).

Again, as reported for 5-HT<sub>1A</sub>R, the introduction of a flexible linker between the spiro-cyclic portion and the phenyl ring allow

ligands to better occupy the receptor binding site. Thus, compounds which combine these two features displayed the higher affinity values of the series (**8**, **12** and **15**). However, a drastic drop of  $\alpha_1$  affinity is observed ( $pK_i\alpha_{1D} < 7.5$ ) compared to the reference ligand

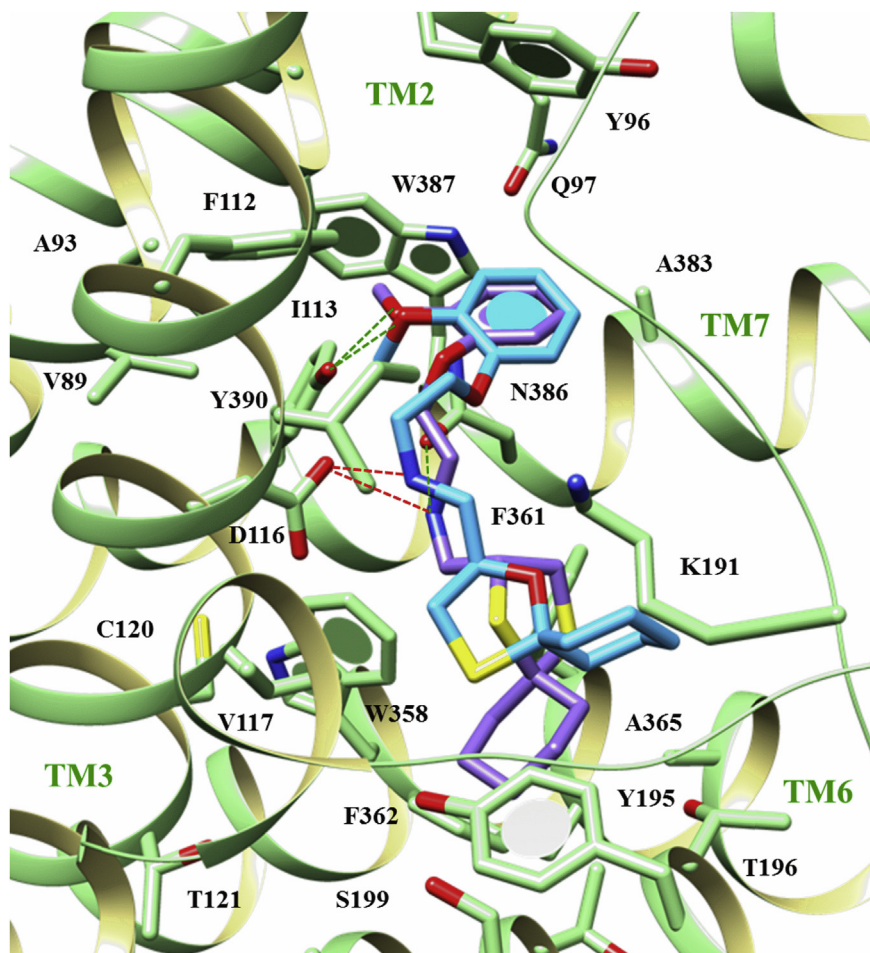


**Fig. 12.** The compound **12** and **15** docking poses into the 5HT<sub>1A</sub> binding site are reported. The ligands are coloured by atom-type (**12** C atom: cyan; **15** C atom: purple). Salt-bridge and H-bond contacts are displayed by line and coloured in red and light green, respectively. (For interpretation of the references to colour in this figure legend, the reader is referred to the web version of this article.)

**A** ( $pK_i\alpha_{1D} = 9.09$ ). According to our results, this is probably related to the introduction of the spiro-decane moiety in place of the diphenyl-substituted ring. In particular, all these compounds oriented the spiro-cyclic portion towards a deep hydrophobic cavity including M156, W172, C246, F384, K385, F388, by detecting Van der Waals contacts. Thus, the phenyl or 2-methoxyphenyl group of the amine chain partially occupies the receptor region delimited by V177, Y254, F364, F365, L368. On this basis, the absence of an aromatic substituent on the spiro-cyclic moiety could cause a reversed ligand binding mode with respect to **A**, guiding the phenyl or methoxy-phenyl group towards Y254, F364, F365 residues. In this way, although a number of  $\pi$ - $\pi$  stacking contacts were conserved, as for **A**, the relevant H-bond interaction with K385 is lost, resulting in lower affinity values.

### 3. Conclusion

In the present work a series of derivatives of **1** were synthesized and tested for binding affinity and activity at 5-HT<sub>1A</sub>R and  $\alpha_1$  adrenoceptors and SAR studies were drawn (Figure 14). In particular we observed that:

- isosteric substitution of the ring oxygen atoms with sulphur favours 5-HT<sub>1A</sub>R affinity, potency and efficacy especially in the presence of a more flexible amine chain;
- compounds **14** and **15** emerged as novel 5-HT<sub>1A</sub>R partial agonists, the first being outstanding for selectivity (5-HT<sub>1A</sub>/ $\alpha_{1D} = 80$ ), the latter for potency ( $pD_2 = 9.58$ ) and efficacy ( $E_{max} = 74\%$ ). Compared to the lead compound **1**, **15** exhibited a 10-fold improved potency and about 50% enhanced efficacy.
- compound **15** demonstrated to permeate the BBB by passive diffusion and showed a promising neuroprotective activity *in vitro*.
- In formalin test compound **15** reduces significantly the linking time in Phase II at a dose of 10 mg/kg i.p. indicating a potent analgesic activity and suggesting an additional and new strategy for pain control.

### 4. Experimental section

#### 4.1. Materials and methods

All reagents, solvents and other chemicals were used as purchased from Sigma-Aldrich without further purification unless otherwise specified. Air- or moisture-sensitive reactants and solvents were employed in reactions carried out under nitrogen atmosphere unless otherwise noted. Flash column chromatography purifications (medium pressure liquid chromatography) were carried out using Merck silica gel 60 (230–400 mesh, ASTM). The purity of compounds was determined by elemental analysis (C,H,N) on a Carlo Erba 1106 Analyzer in the Microanalysis Laboratory of

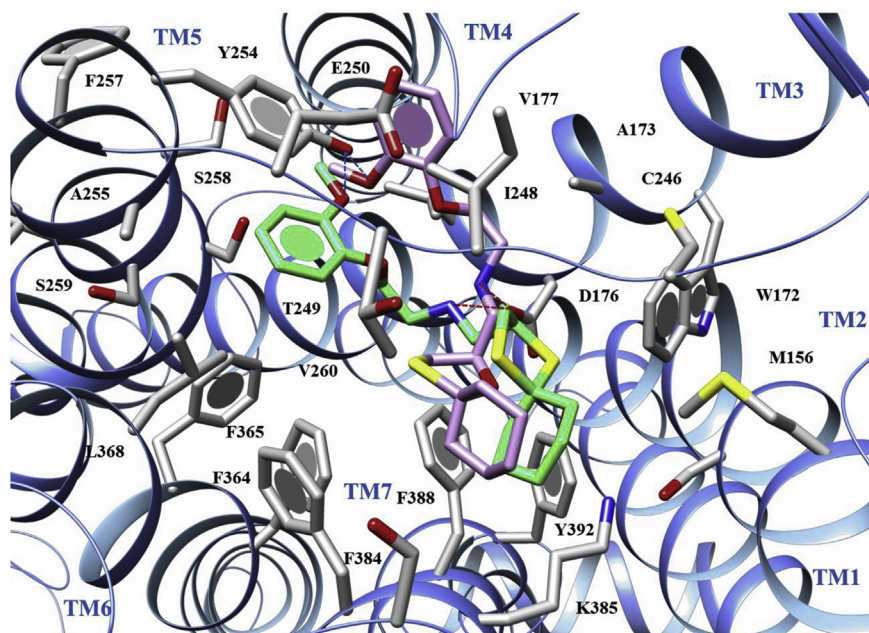


**Fig. 13.** The compound **12** and **15** docking pose into the final  $\alpha_{1D}$  binding site are reported. The ligand is coloured by atom-type (**12** C atom: light purple; **15** C atom: light green). Salt-bridge and H-bond contacts are displayed by line and coloured in red and light blue, respectively. (For interpretation of the references to colour in this figure legend, the reader is referred to the web version of this article.)

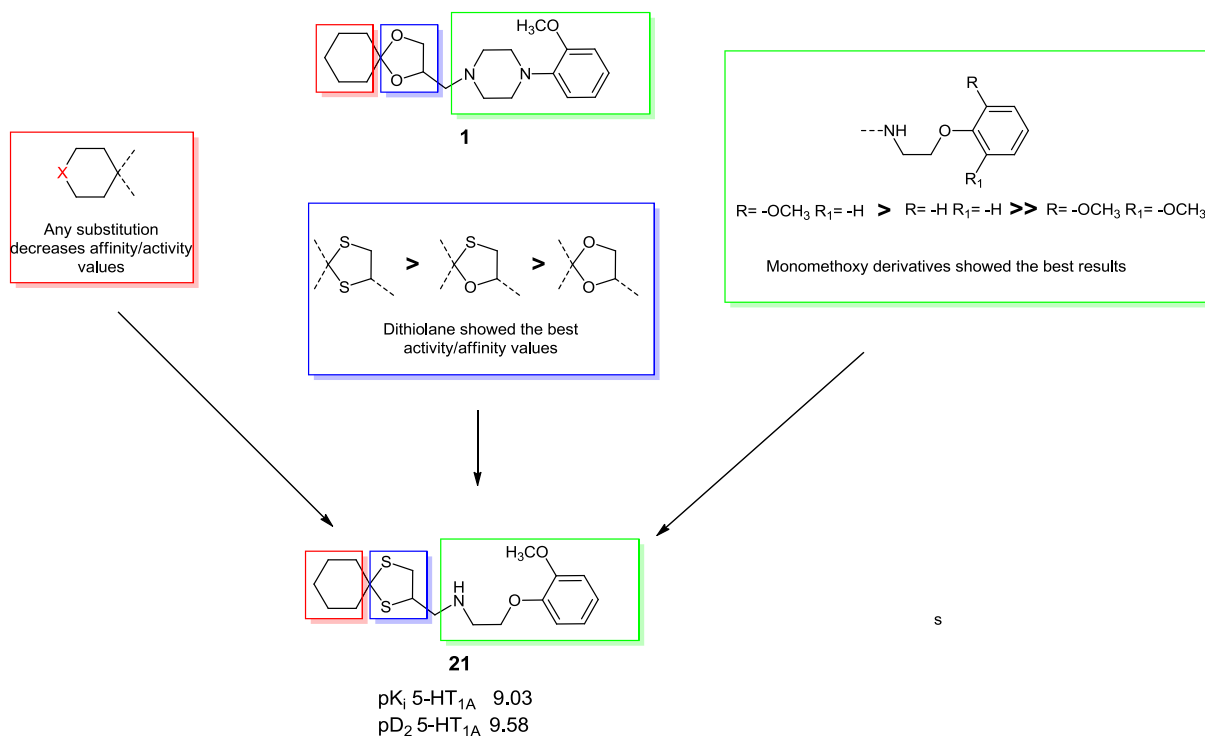


**Fig. 14.** SAR milestones of compound **1**.

the Life Sciences Department of Università degli Studi di Modena e Reggio Emilia and the results are within  $\pm 0.4\%$  of the theoretical values. Melting points were determined with a Stuart SMP3 in open capillaries and they are uncorrected. The structures of all isolated compounds were confirmed by Nuclear magnetic resonance (NMR) and Mass spectrometry.  $^1\text{H}$  and  $^{13}\text{C}$  NMR (1D and 2D experiments)

spectra were recorded on a DPX-200/400 Avance (Bruker) spectrometer at 200 MHz and 400 MHz respectively and on AVANCE III (Bruker Biospin) at 600 MHz. Chemical shifts are expressed in  $\delta$  (ppm).  $^1\text{H}$  NMR chemical shifts are relative to tetramethylsilane (TMS) as internal standard.  $^{13}\text{C}$  NMR chemical shifts are relative to TMS at  $\delta$  0.0 or to the  $^{13}\text{C}$  signal of the solvent:  $\text{CDCl}_3 \delta$  77.04,  $\text{CD}_3\text{OD}$

$\delta$  49.8, DMSO- $d_6$   $\delta$  39.5. NMR data are reported as follows: chemical shift, number of protons/carbons, multiplicity (s, singlet; d, doublet; t, triplet; q, quartet; m, multiplet; br, broadened), coupling constants (Hz) and assignment (Dosd = 1,4-dioxaspiro[4.5]decane; Ph = phenyl; Otsd = 1-oxa-4-thiaspiro[4.5]decane, Ts = tosyl; Arom = aromatic; Piperaz = piperazine; Dtsd = 1,4-dithiaspiro[4.5]decane).  $^1\text{H}$ – $^1\text{H}$  correlation spectroscopy (COSY),  $^1\text{H}$ – $^{13}\text{C}$  heteronuclear multiple quantum coherence (HMQC) and heteronuclear multiple bond connectivity (HMBC) experiments were recorded for determination of  $^1\text{H}$ – $^1\text{H}$  and  $^1\text{H}$ – $^{13}\text{C}$  correlations respectively. Mass spectra were obtained on a hybrid QTOF mass spectrometer (PE SCIEX-QSTAR) using electrospray ionization mode (HR-ESI-MS, ion voltage of 4800 V). The HPLC experimental conditions of the HPLC-MS system are: flow rate 5 mL/min, sample solution (10 pmol/mL) of the selected compound with 0.1% acetic acid, mobile phase consisting of methanol (50%) and water (50%). The yields reported are based on a single experiment and are not optimized. The oxalate salts of all tested compounds were used for the pharmacological evaluations.

The compounds **4** and **7** were obtained as previously reported [40].

#### 4.2. 1-Oxa-4-thiaspiro[4.5]decan-2-ylmethanol (**2**)

A round-bottom flask was charged with cyclohexanone (2 g, 20.0 mmol), 3-mercapto propane-1,2-diol (2.60 g, 24.0 mmol) and (0.5 mmol/g)  $\text{HClO}_4/\text{SiO}_2$  (0.4 g). The reaction mixture was stirred at room temperature, under nitrogen, for 6 h. Then the reaction mixture was diluted with EtOAc and then filtered and evaporated under reduced pressure. Purification by flash chromatography (85/15 Cy/EtAc) afforded the title compound as brown oil [47].

Yield 3.05 g (16.0 mmol, 81%).  $^1\text{H}$  NMR (400 MHz,  $\text{CDCl}_3$ ):  $\delta$  1.18–1.33 (m, 1H, CHa-8 Otsd), 1.36–1.57 (m, 3H, CHb-8, CHa-7, CHa-9 Otsd), 1.65–1.99 (m, 6H, CHb-7, CHb-9, CH<sub>2</sub>-6, CH<sub>2</sub>-10 Otsd), 2.92 (dd,  $J$  = 9.1, 10.3 Hz, 1H, CHa-3 Otsd), 2.98 (dd,  $J$  = 5.4, 10.3 Hz, 1H, CHb-3 Otsd), 3.68 (dd,  $J$  = 5.3, 11.6 Hz, 1H, CHaOH), 3.81 (dd,  $J$  = 3.5, 11.6 Hz, 1H, CHbOH), 4.28–4.39 (m, 1H, CH-2 Otsd).  $^{13}\text{C}$  NMR (100 MHz,  $\text{CDCl}_3$ ):  $\delta$  23.9 (CH<sub>2</sub>, C-8 Otsd), 24.7 (CH<sub>2</sub>, C-7/C-9 Otsd), 25.0 (CH<sub>2</sub>, C-7/C-9 Otsd), 33.1 (CH<sub>2</sub>, C-3 Otsd), 39.7 (CH<sub>2</sub>, C-6/C-10 Otsd), 40.1 (CH<sub>2</sub>, C-6/C-10 Otsd), 63.3 (CH<sub>2</sub>, CH<sub>2</sub>OH), 81.3 (CH, C-2 Otsd), 96.4 (C, C-5 Otsd).

#### 4.3. 1,4-Dithiaspiro[4.5]decan-2-ylmethanol (**3**)

The title compound [47] was obtained from cyclohexanone and 2,3-dimercaptopropan-1-ol following the procedure described for **2**.

Yield 2.90 g (14.0 mmol, 71%).  $^1\text{H}$  NMR (400 MHz,  $\text{CDCl}_3$ )  $\delta$  1.22–1.39 (m, 2H, CH<sub>2</sub>-8 Dtsd), 1.33–1.79 (m, 4H, CH<sub>2</sub>-7, CH<sub>2</sub>-9 Dtsd), 1.81–2.14 (m, 4H, CH<sub>2</sub>-6, CH<sub>2</sub>-10 Dtsd), 3.26–3.41 (m, 2H, CH<sub>2</sub>-3 Dtsd), 3.62 (dd,  $J$  = 5.1, 11.7 Hz, 1H, CHaOH), 3.77 (dd,  $J$  = 3.6, 11.7 Hz, 1H, CHbOH), 3.84–3.96 (m, 1H, CH-2 Dtsd).  $^{13}\text{C}$  NMR (100 MHz,  $\text{CDCl}_3$ ):  $\delta$  22.6 (CH<sub>2</sub>, C-8 Dtsd), 25.3 (CH<sub>2</sub>, C-7/C-9 Dtsd), 25.9 (CH<sub>2</sub>, C-7/C-9 Dtsd), 35.3 (CH<sub>2</sub>, C-3 Dtsd), 37.2 (CH<sub>2</sub>, C-6/C-10 Dtsd), 37.6 (CH<sub>2</sub>, C-6/C-10 Dtsd), 52.3 (CH, C-2 Dtsd), 58.6 (C, C-5 Dtsd), 61.9 (CH<sub>2</sub>, CH<sub>2</sub>OH).

#### 4.4. 1-Oxa-4-thiaspiro[4.5]decan-2-ylmethyl 4-methylbenzenesulfonate (**5**)

To a solution of **2** (1.5 g, 7.98 mmol) and  $\text{Et}_3\text{N}$  (1.11 mL, 7.98 mmol) in  $\text{CH}_2\text{Cl}_2$  (10 mL) tosyl chloride (2.43 g, 18.0 mmol) was added at 0 °C. The resulting mixture was stirred at room temperature, under nitrogen for 6 h and then the solvent was evaporated. The residue was taken up with EtOAc and washed with saturated

solution sodium bicarbonate and brine. The organic layer was dried over anhydrous sodium sulfate, filtered and concentrated in vacuum. Purification by flash chromatography (gradient from 99/1 to 70/30 Cy/EtAc) afforded the title compound as yellow oil.

Yield 2.25 g, (6.57 mmol, 82%).  $^1\text{H}$  NMR (400 MHz,  $\text{CDCl}_3$ ):  $\delta$  1.22–1.36 (m, 1H, CHa-8 Otsd), 1.36–1.57 (m, 3H, CHb-8, CHa-7, CHa-9 Otsd), 1.63–1.94 (m, 6H, CHb-7, CHb-9, CH<sub>2</sub>-6, CH<sub>2</sub>-10 Otsd), 2.49 (s, 3H, CH<sub>3</sub> Ts) 2.83 (dd,  $J$  = 8.0, 10.7 Hz, 1H, CHa-3 Otsd), 3.09 (dd,  $J$  = 5.3, 10.7 Hz, 1H, CHb-3 Otsd), 4.09–4.22 (m, 2H, CH<sub>2</sub>OH), 4.39–4.51 (m, 1H, CH-2 Otsd), 7.39 (d,  $J$  = 8.1 Hz, 2H, CH-3, CH-5 Ts), 7.84 (d,  $J$  = 8.1 Hz, 2H, CH-2, CH-6 Ts).  $^{13}\text{C}$  NMR (100 MHz,  $\text{CDCl}_3$ ):  $\delta$  21.4 (CH<sub>3</sub>, CH<sub>3</sub> Ts), 24.0 (CH<sub>2</sub>, C-8 Otsd), 24.7 (CH<sub>2</sub>, C-7/C-9 Otsd), 25.0 (CH<sub>2</sub>, C-7/C-9 Otsd), 33.9 (CH<sub>2</sub>, C-3 Otsd), 39.7 (CH<sub>2</sub>, C-6/C-10 Otsd), 40.1 (CH<sub>2</sub>, C-6/C-10 Otsd), 69.6 (CH<sub>2</sub>, CH<sub>2</sub>OH), 78.0 (CH, C-2 Otsd), 96.9 (C, C-5 Otsd), 127.7 (2 CH, C-2, C-6 Ts), 129.6 (2 CH, C-3, C-5 Ts), 132.5 (C, C-1 Ts), 147.7 (C, C-4 Ts). HRMS-APCI  $m/z$  [M+H]<sup>+</sup> calcd for  $\text{C}_{16}\text{H}_{23}\text{O}_4\text{S}_2$ : 343.1032; found 343.1032.

#### 4.5. 2-(Chloromethyl)-1,4-dithiaspiro[4.5]decane (**6**)

To a solution of **3** (2.9 g, 14.2 mmol), in toluene (15 mL) thionyl chloride (1.35 mL, 18.5 mmol) was added at 0 °C. The resulting mixture was stirred at 80 °C for 12 h and then the solvent was evaporated. The residue solubilized in EtOAc was washed with saturated solution of sodium bicarbonate and brine. The organic phase was dried over anhydrous sodium sulfate, filtered and evaporated. Purification by flash chromatography (99/1 Cy/EtAc) afforded the title compound as dark oil.

Yield 0.93 g (4.19 mmol, 30%).  $^1\text{H}$  NMR (400 MHz,  $\text{CDCl}_3$ ):  $\delta$  1.31–1.52 (m, 2H, CH<sub>2</sub>-8 Dtsd), 1.57–1.84 (m, 4H, CH<sub>2</sub>-7, CH<sub>2</sub>-9 Dtsd), 1.94–2.07 (m, 4H, CH<sub>2</sub>-6, CH<sub>2</sub>-10 Dtsd), 3.39 (dd,  $J$  = 4.6, 12.5 Hz, 1H, CHa-3 Dtsd), 3.47 (dd,  $J$  = 2.6, 12.5 Hz, 1H, CHb-3 Dtsd), 3.54 (dd,  $J$  = 3.7, 10.3 Hz, 1H, CHaCl), 3.84 (dd,  $J$  = 10.3, 10.9 Hz, 1H, CHbCl), 3.88–3.97 (m, 1H, CH-2 Dtsd).  $^{13}\text{C}$  NMR (100 MHz,  $\text{CDCl}_3$ ):  $\delta$  24.6 (CH<sub>2</sub>, C-8 Dtsd), 25.2 (CH<sub>2</sub>, C-7/C-9 Dtsd), 26.5 (CH<sub>2</sub>, C-7/C-9 Dtsd), 38.9 (CH<sub>2</sub>, C-3 Dtsd), 42.0 (CH<sub>2</sub>, C-6/C-10 Dtsd), 43.0 (CH<sub>2</sub>, C-6/C-10 Dtsd), 45.1 (CH<sub>2</sub>, CH<sub>2</sub>Cl), 55.0 (CH, C-2 Dtsd), 69.1 (C, C-5 Dtsd). HRMS-APCI  $m/z$  [M+H]<sup>+</sup> calcd for  $\text{C}_9\text{H}_{16}\text{ClS}_2$ : 223.0376; found 223.0378.

#### 4.6. General procedure for the synthesis of the amines **8**–**15**

A 10 mL microwave vial was charged with **4** or **5** or **6** (1.0 mmol), a small excess (1.2 mmol) of 2-phenoxy- or (2-methoxyphenoxy)- or (2,6-dimethoxyphenoxy)-ethanamine and a catalytic amount of potassium iodide in 1 mL of 2-methoxyethanol. The reaction was stirred under microwave irradiation at 160 °C (pressure 100 PSI, power 50 W) for 30 min. Then the solvent was evaporated under reduced pressure. The residue was taken up with EtOAc, basified with 5% NaOH. The organic layer was dried over anhydrous sodium sulfate, filtered and evaporated under reduced pressure. The residue was purified by flash column chromatography.

##### 4.6.1. N-(1,4-Dioxaspiro[4.5]decan-2-ylmethyl)-2-(2-methoxyphenoxy)ethanamine (**8**)

The title compound was purified by flash chromatography on silica gel cartridge (80/20/5 Cy/EtAc/MeOH + 2  $\text{NH}_4\text{OH}$ ) to afford 0.111 g (0.34 mmol, 54%) of **8** as yellow oil.

$^1\text{H}$  NMR (400 MHz,  $\text{CDCl}_3$ ):  $\delta$  1.31–1.52 (m, 2H, CH<sub>2</sub>-8 Dosd), 1.49–1.79 (m, 8H, CH<sub>2</sub>-7, CH<sub>2</sub>-9, CH<sub>2</sub>-6, CH<sub>2</sub>-10 Dosd), 2.66–2.95 (m, 2H, CH<sub>2</sub>N), 3.07 (t,  $J$  = 5.5 Hz, 2H, CH<sub>2</sub>CH<sub>2</sub>O), 3.69 (dd,  $J$  = 7.4, 7.9 Hz, 1H, CHa-3 Dosd), 3.86 (s, 3H, OCH<sub>3</sub>), 4.01–4.19 (m, 3H, CHb-3 Dosd, CH<sub>2</sub>O), 4.19–4.36 (m, 1H, CH-2 Dosd), 6.73–7.08 (m, 4H, CH-3, CH-4, CH-5, CH-6 Ph).  $^{13}\text{C}$  NMR (100 MHz,  $\text{CDCl}_3$ ):  $\delta$  23.6 (CH<sub>2</sub>, C-8 Dosd), 24.1 (CH<sub>2</sub>, C-7/C-9 Dosd), 25.2 (CH<sub>2</sub>, C-7/C-9 Dosd), 34.3

(CH<sub>2</sub>, C-6/C-10 Dosd), 36.4 (CH<sub>2</sub>, C-6/C-10 Dosd), 48.1 (CH<sub>2</sub>, CH<sub>2</sub>CH<sub>2</sub>O), 51.7 (CH<sub>2</sub>, CHCH<sub>2</sub>N), 67.0 (CH<sub>2</sub>, C-3 Dosd), 73.0 (CH<sub>2</sub>, CH<sub>2</sub>O), 74.6 (CH, C-2 Dosd), 109.5 (C, C-5 Dosd), 111.9 (CH, C-3 Ph), 114.4 (CH, C-5 Ph), 120.6 (CH, C-6 Ph), 121.7 (CH, C-4 Ph), 148.1 (C, C-1 Ph), 149.7 (C, C-2 Ph).

The free amine (0.100 g, 0.31 mmol) was dissolved in Et<sub>2</sub>O and treated with 1.2 eq. of oxalic acid to give 0.083 g (0.20 mmol, 64% yield) of the corresponding oxalate salt.

Mp: 201–203 °C. <sup>1</sup>H NMR (600 MHz, DMSO-*d*<sub>6</sub>): δ 1.25–1.44 (m, 2H, CH<sub>2</sub>-8), 1.45–1.68 (m, 8H, CH<sub>2</sub>-7, CH<sub>2</sub>-9, CH<sub>2</sub>-6, CH<sub>2</sub>-10 Dosd), 3.13 (dd, *J* = 2.8, 4.2 Hz, 1H, CHCH<sub>2</sub>N), 3.18–3.29 (m, 3H, CHCH<sub>2</sub>N, CH<sub>2</sub>CH<sub>2</sub>O), 3.74 (dd, *J* = 1.8, 2.8 Hz, 1H, CHa-3 Dosd), 3.80 (s, 3H, OCH<sub>3</sub>), 4.05–4.14 (m, 3H, CH<sub>2</sub>O, CHb-3 Dosd), 4.37–4.44 (m, 1H, CH-2 Dosd), 6.87–7.05 (m, 4H, CH-3, CH-4, CH-5, CH-6 Ph). HRMS-ESI *m/z* [M+H]<sup>+</sup> calcd for C<sub>18</sub>H<sub>28</sub>NO<sub>4</sub>: 322.2013; found 322.2016. Anal. calcd for C<sub>20</sub>H<sub>29</sub>NO<sub>8</sub>: C 58.38, H 7.10, N 3.40; found: C 58.62, H 7.27, N 3.49.

#### 4.6.2. *N*-(1,4-Dioxaspiro[4.5]decan-2-ylmethyl)-2-(2,6-dimethoxyphenoxy)ethanamine (**9**)

The title compound was purified by flash column chromatography on silica gel (gradient from 30/70 to 100 Cy/EtAc) to afford 0.165 g (0.47 mmol, 54%) of **9** as oil.

<sup>1</sup>H NMR (400 MHz, CDCl<sub>3</sub>): δ 1.34–1.50 (m, 2H, CH<sub>2</sub>-8 Dosd), 1.52–1.82 (m, 8H, CH<sub>2</sub>-7, CH<sub>2</sub>-9, CH<sub>2</sub>-6, CH<sub>2</sub>-10 Dosd), 2.91 (d, *J* = 5.9 Hz, 2H, CHCH<sub>2</sub>N), 3.02 (t, *J* = 5.4 Hz, 2H, CH<sub>2</sub>CH<sub>2</sub>O), 3.74 (dd, *J* = 6.3, 8.1 Hz, CHa-3 Dosd), 3.90 (s, 6H, 2 x OCH<sub>3</sub>), 4.06–4.19 (m, 3H, CHb-3 Dosd, CH<sub>2</sub>O), 4.35–4.47 (m, 1H, CH-2 Dosd), 6.61 (d, *J* = 7.4 Hz, 2H, CH-3, CH-5 Ph), 7.04 (t, *J* = 7.4 Hz, CH-4 Ph). <sup>13</sup>C NMR (100 MHz, CDCl<sub>3</sub>): δ = 23.5 (CH<sub>2</sub>, C-8 Dosd), 23.7 (CH<sub>2</sub>, C-7/C-9 Dosd), 24.9 (CH<sub>2</sub>, C-7/C-9 Dosd), 34.7 (CH<sub>2</sub>, C-6/C-10 Dosd), 36.4 (CH<sub>2</sub>, C-6/C-10 Dosd), 49.3 (CH<sub>2</sub>, CH<sub>2</sub>CH<sub>2</sub>O), 52.1 (CH<sub>2</sub>, CHCH<sub>2</sub>N), 55.8 (2 CH<sub>3</sub>, OCH<sub>3</sub>), 67.0 (CH<sub>2</sub>, C-3 Dosd), 71.4 (CH<sub>2</sub>, CH<sub>2</sub>O), 74.3 (CH, C-2 Dosd), 104.9 (2 CH, C-3, C-5 Ph), 109.7 (C, C-5 Dosd), 123.7 (CH, C-4 Ph), 136.3 (C, C-1 Ph), 153.3 (2 C, C-2, C-6 Ph).

The free amine (0.150 g, 0.42 mmol) was dissolved in Et<sub>2</sub>O and treated with 1.2 eq. of oxalic acid to give 0.108 g (0.24 mmol, 58% yield) of the corresponding oxalate salt.

Mp: 182–184 °C. <sup>1</sup>H NMR (600 MHz, DMSO-*d*<sub>6</sub>): δ 1.29–1.42 (m, 2H, CH<sub>2</sub>-8), 1.47–1.63 (m, 8H, CH<sub>2</sub>-7, CH<sub>2</sub>-9, CH<sub>2</sub>-6, CH<sub>2</sub>-10 Dosd), 3.10 (dd, *J* = 2.9, 4.3 Hz, 1H, CHCH<sub>2</sub>N), 3.20–3.30 (m, 3H, CHCH<sub>2</sub>N, CH<sub>2</sub>CH<sub>2</sub>O), 3.74 (dd, *J* = 1.9, 2.9 Hz, 1H, CHa-3 Dosd), 3.79 (s, 6H, OCH<sub>3</sub>), 4.06–4.13 (m, 3H, CH<sub>2</sub>O, CHb-3 Dosd), 4.41 (m, 1H, CH-2 Dosd), 6.71 (d, 2H, *J* = 8.5 Hz, CH-3, CH-5 Ph), 7.06 (t, *J* = 8.3 Hz, 1H, CH-4 Ph). HRMS-ESI *m/z* [M+H]<sup>+</sup> calcd for C<sub>19</sub>H<sub>30</sub>NO<sub>5</sub>: 352.2118; found 352.2126. Anal. calcd for C<sub>21</sub>H<sub>31</sub>NO<sub>9</sub>: C 57.13, H 7.08, N 3.17; found: C 57.42, H 7.31, N 3.44.

#### 4.6.3. 1-(1-Oxa-4-thiaspiro[4.5]decan-2-ylmethyl)-4-(2-methoxyphenyl)piperazine (**10**)

The title compound was purified by flash chromatography on silica gel cartridge (80/20 Cy/EtAc) to afford 0.178 g (0.49 mmol, 67% of **10** as oil.

<sup>1</sup>H NMR (400 MHz, CDCl<sub>3</sub>): δ 1.23–1.41 (m, 1H, CHa-8 Otsd), 1.42–1.60 (m, 3H, CHb-8, CHa-7, CHa-9 Otsd), 1.67–2.04 (m, 6H, CHb-7, CHb-9, CH<sub>2</sub>-6, CH<sub>2</sub>-10 Otsd), 2.67–2.97 (m, 7H, CH<sub>2</sub>-N, CH<sub>2</sub>-2, CH<sub>2</sub>-6 Piperaz, CHa-3 Otsd), 3.08–3.27 (m, 5H, CH<sub>2</sub>-3, CH<sub>2</sub>-5 piperaz, CHb-3 Otsd), 3.90 (s, 3H, OCH<sub>3</sub>), 4.43–4.56 (m, 1H, CH-2 Otsd), 6.90 (d, *J* = 7.9 Hz, 1H, CH-3 Arom), 6.93–7.02 (m, 2H, CH-5, CH-6 Arom), 7.04–7.16 (m, 1H, CH-4 Arom). <sup>13</sup>C NMR (100 MHz, CDCl<sub>3</sub>): δ 24.1 (CH<sub>2</sub>, C-8 Otsd), 24.8 (CH<sub>2</sub>, C-7/C-9 Otsd), 25.1 (CH<sub>2</sub>, C-7/C-9 Otsd), 36.4 (CH<sub>2</sub>, C-3 Otsd), 39.9 (CH<sub>2</sub>, C-6/C-10 Otsd), 40.5 (CH<sub>2</sub>, C-6/C-10 Otsd), 50.2 (2 CH<sub>2</sub>, C-3, C-5 Piperaz), 53.8 (2 CH<sub>2</sub>, C-2, C-6 Piperaz), 55.1 (CH<sub>3</sub>, OCH<sub>3</sub>), 61.4 (CH<sub>2</sub>, CH<sub>2</sub>N), 79.2 (CH, C-2 Otsd), 96.4 (C, C-5 Otsd), 110.9 (CH, C-3 Arom), 117.9 (CH, C-5 Arom),

120.7 (CH, C-6 Arom), 122.7 (CH, C-4 Arom), 141.0 (C, C-1 Arom), 152.0 (C, C-2 Arom).

The free amine (0.178 g, 0.49 mmol) was dissolved in Et<sub>2</sub>O and treated with 1.2 eq. of oxalic acid to give 0.174 g (0.38 mmol, 79% yield) of the corresponding oxalate salt.

Mp: 217–218 °C. <sup>1</sup>H NMR (600 MHz, DMSO-*d*<sub>6</sub>): δ 1.25–1.48 (m, 4H, CH<sub>2</sub>-8, CHa-7, CHa-9 Otsd), 1.62–1.94 (m, 6H, CHb-7, CHb-9, CH<sub>2</sub>-6, CH<sub>2</sub>-10 Otsd), 2.81 (dd, *J* = 9.4, 10.3 Hz, 1H, CHa-3 Otsd), 3.11–3.32 (m, 11H, CH<sub>2</sub>-2, CH<sub>2</sub>-3, CH<sub>2</sub>-5, CH<sub>2</sub>-6 Piperaz, CHb-3 Otsd, CH<sub>2</sub>N), 3.79 (s, 3H, OCH<sub>3</sub>), 4.55–4.62 (m, 1H, CH-2), 6.87–7.02 (m, 4H, Arom). HRMS-ESI *m/z* [M+H]<sup>+</sup> calcd for C<sub>20</sub>H<sub>31</sub>N<sub>2</sub>O<sub>2</sub>S<sup>+</sup>: 363.2106; found 363.2103. Anal. calcd for C<sub>22</sub>H<sub>32</sub>N<sub>2</sub>O<sub>6</sub>S: C 58.39, H 7.13, N 6.19; found: C 58.44, H 7.27, N 6.24.

#### 4.6.4. {1-Oxa-4-thiaspiro[4.5]decan-2-ylmethyl}(2-phenoxyethyl)amine (**11**)

The title compound was purified by flash chromatography on silica gel cartridge (80/20 Cy/EtAc) to afford 0.056 g (0.18 mmol, 25%) of **11** as yellow oil.

<sup>1</sup>H NMR (400 MHz, CDCl<sub>3</sub>): δ 1.21–1.39 (m, 1H, CHa-8 Otsd), 1.43–1.61 (m, 3H, CHb-8, CHa-7, CHa-9 Otsd), 1.73–2.01 (m, 6H, CHb-7, CHb-9, CH<sub>2</sub>-6, CH<sub>2</sub>-10 Otsd), 2.85 (dd, *J* = 9.2, 10.0 Hz, 1H, CHa-3 Otsd), 2.91–3.06 (m, 2H, CHCH<sub>2</sub>NH), 3.09 (dd, *J* = 5.0, 10.0 Hz, 1H, CHb-3 Otsd), 3.14 (d, *J* = 5.3 Hz, 2H, NHCH<sub>2</sub>CH<sub>2</sub>), 4.09 (t, *J* = 5.3 Hz, 2H, CH<sub>2</sub>O), 4.42–4.51 (m, 1H, CH-2 Otsd), 6.82–7.12 (m, 3H, CH-2, CH-4, CH-6 Ph), 7.21–7.48 (m, 2H, CH-3, CH-5 Ph). <sup>13</sup>C NMR (100 MHz, CDCl<sub>3</sub>): δ 24.0 (CH<sub>2</sub>, C-8 Otsd), 24.8 (CH<sub>2</sub>, C-7/C-9 Otsd), 25.1 (CH<sub>2</sub>, C-7/C-9 Otsd), 35.3 (CH<sub>2</sub>, C-3 Otsd), 39.9 (CH<sub>2</sub>, C-6/C-10 Otsd), 40.4 (CH<sub>2</sub>, C-6/C-10 Otsd), 48.7 (CH<sub>2</sub>, NCH<sub>2</sub>CH<sub>2</sub>), 52.6 (CH<sub>2</sub>, CHCH<sub>2</sub>N), 66.8 (CH<sub>2</sub>, CH<sub>2</sub>O), 80.4 (CH, C-2 Otsd), 96.3 (C, C-5 Otsd), 114.3 (2 CH, C-2, C-6 Ph), 120.6 (CH, C-4 Ph), 129.2 (2 CH, C-3, C-5 Ph), 158.5 (C, C-1 Ph).

The free amine (0.057 g, 0.186 mmol) was dissolved in Et<sub>2</sub>O and treated with 1.2 eq. of oxalic acid to give 0.067 g (0.169 mmol, 91% yield) of the corresponding oxalate salt.

Mp: 210–211 °C. <sup>1</sup>H NMR (600 MHz, DMSO-*d*<sub>6</sub>): δ 1.20–1.52 (m, 4H, CH<sub>2</sub>-8, CHa-7, CHa-9 Otsd), 1.64–1.93 (m, 6H, CHb-7, CHb-9, CH<sub>2</sub>-6, CH<sub>2</sub>-10 Otsd), 2.83 (dd, *J* = 8.5, 10.6 Hz, 1H, CHa-3 Otsd), 3.14–3.22 (m, 2H, CHb-3 Otsd, CHCH<sub>2</sub>N), 3.31–3.42 (m, 3H, CHCH<sub>2</sub>N, NCH<sub>2</sub>CH<sub>2</sub>), 4.25 (t, *J* = 4.9 Hz, 2H, CH<sub>2</sub>O), 4.52 (m, 1H, CH-2 Otsd), 6.99 (m, 3H, CH-2, CH-4, CH-6 Ph), 7.32 (m, 2H, CH-3, CH-5 Ph). HRMS-ESI *m/z* [M+H]<sup>+</sup> calcd for C<sub>17</sub>H<sub>26</sub>NO<sub>2</sub>S<sup>+</sup>: 308.1679; found 308.1675. Anal. calcd for C<sub>19</sub>H<sub>27</sub>NO<sub>6</sub>S: C 57.41, H 6.85, N 3.52, found: C 57.62, H 6.94, N 3.66.

#### 4.6.5. *N*-(1-Oxa-4-thiaspiro[4.5]decan-2-ylmethyl)-2-(2-methoxyphenoxy)ethanamine (**12**)

The title compound was purified by flash chromatography on silica gel cartridge (70/30/10 Cy/EtAc/MeOH + 1 NH<sub>4</sub>OH) to afford 0.046 g (0.14 mmol, 19%) of **12** as yellow oil.

<sup>1</sup>H NMR (400 MHz, CDCl<sub>3</sub>): δ 1.23–1.38 (m, 1H, CHa-8 Otsd), 1.41–1.58 (m, 3H, CHb-8, CHa-7, CHa-9 Otsd), 1.69–2.00 (m, 6H, CHb-7, CHb-9, CH<sub>2</sub>-6, CH<sub>2</sub>-10 Otsd), 2.86 (dd, *J* = 9.1, 9.9 Hz, 1H, CHa-3 Otsd), 3.01 (d, *J* = 5.4 Hz, 2H, CHCH<sub>2</sub>N), 3.09 (dd, *J* = 5.0, 9.9 Hz, 1H, CHb-3), 3.15 (dt, *J* = 1.3, 5.2 Hz, 2H, NCH<sub>2</sub>CH<sub>2</sub>), 3.90 (s, 3H, OCH<sub>3</sub>), 4.19 (t, *J* = 5.2 Hz, 2H, CH<sub>2</sub>O), 4.39–4.50 (m, 1H, CH-2 Otsd), 6.72–7.04 (m, 4H, Ph). <sup>13</sup>C NMR (100 MHz, CDCl<sub>3</sub>): δ 24.0 (CH<sub>2</sub>, C-8 Otsd), 24.8 (CH<sub>2</sub>, C-7/C-9 Otsd), 25.1 (CH<sub>2</sub>, C-7/C-9 Otsd), 35.3 (CH<sub>2</sub>, C-3 Otsd), 39.9 (CH<sub>2</sub>, C-6/C-10 Otsd), 40.4 (CH<sub>2</sub>, C-6/C-10 Otsd), 48.5 (CH<sub>2</sub>, NCH<sub>2</sub>CH<sub>2</sub>), 52.5 (CH<sub>2</sub>, CHCH<sub>2</sub>N), 55.6 (CH<sub>3</sub>, OCH<sub>3</sub>), 68.4 (CH<sub>2</sub>, CH<sub>2</sub>O), 80.2 (CH, C-2 Otsd), 96.3 (C, C-5 Otsd), 111.8 (CH, C-3 Ph), 114.3 (CH, C-5 Ph), 120.7 (CH, C-6 Ph), 121.5 (CH, C-4 Ph), 148.0 (C, C-1 Ph), 149.6 (C, C-2 Ph).

The free amine (0.046 g, 0.137 mmol) was dissolved in Et<sub>2</sub>O and treated with 1.2 eq. of oxalic acid to give 0.048 g (0.159 mmol, 83%

yield) of the corresponding oxalate salt.

Mp: 202–203 °C. <sup>1</sup>H NMR (600 MHz, DMSO-*d*<sub>6</sub>) δ 1.23–1.48 (m, 4H, CH<sub>2</sub>-8, CHa-7, CHa-9 Otsd), 1.66–1.89 (m, 6H, CHb-7, CHb-9, CH<sub>2</sub>-6, CH<sub>2</sub>-10 Otsd), 2.82 (dd, *J* = 9.2, 10.0 Hz, 1H, CHa-3 Otsd), 3.17 (dd, *J* = 4.5, 10.0 Hz, 1H, CHb-3 Otsd), 3.24 (dd, *J* = 8.1, 12.4 Hz, 1H, CHCHaN), 3.31–3.40 (m, 3H, CHCHbN, NCH<sub>2</sub>CH<sub>2</sub>), 3.78 (s, 3H, OCH<sub>3</sub>), 4.23 (t, *J* = 5.2 Hz, 2H, CH<sub>2</sub>O), 4.52 (m, 1H, CH-2 Otsd), 6.88–7.05 (m, 4H, Ph). HRMS-ESI *m/z* [M+H]<sup>+</sup> calcd for C<sub>18</sub>H<sub>28</sub>NO<sub>3</sub>S<sup>+</sup>: 338.1784; found 338, 1797. Anal. calcd for C<sub>20</sub>H<sub>29</sub>NO<sub>7</sub>S: C 56.19, H 6.84, N 3.28; found: C 56.28, H 6.99, N 3.37.

#### 4.6.6. 1-[1,4-Dithiaspiro[4.5]decan-2-ylmethyl]-4-(2-methoxyphenyl)piperazine (**13**)

The title compound was purified by flash chromatography on silica gel cartridge (90/10 Cy/EtAc) to afford 0.136 g (0.36 mmol, 53%) of **13** as dark oil.

<sup>1</sup>H NMR (400 MHz, CDCl<sub>3</sub>) δ = 1.33–1.51 (m, 2H, CH<sub>2</sub>-8 Dtsd), 1.53–1.81 (m, 4H, CH<sub>2</sub>-7, CH<sub>2</sub>-9 Dtsd), 1.92–2.09 (m, 4H, CH<sub>2</sub>-6, CH<sub>2</sub>-10 Dtsd), 2.47–2.77 (m, 7H, CH<sub>2</sub>-N, CH<sub>2</sub>-2, CH<sub>2</sub>-6 Piperaz, CHa-3 Dtsd), 3.01–3.25 (m, 5H, CH<sub>2</sub>-3, CH<sub>2</sub>-5 Piperaz, CHb-3 Dtsd), 3.25–3.47 (m, 2H, CH<sub>2</sub>-3 Dtsd), 3.85 (m, 3H, OCH<sub>3</sub>), 3.87–3.99 (m, 1H, CH-2 Dtsd), 6.90 (d, *J* = 8.0 Hz, 1H, CH-3 Arom), 6.91–7.05 (m, 2H, CH-5, CH-6 Arom), 7.06–7.15 (m, 1H, CH-4 Arom). <sup>13</sup>C NMR (100 MHz, CDCl<sub>3</sub>): δ 24.1 (CH<sub>2</sub>, C-8 Dtsd), 25.0 (CH<sub>2</sub>, C-7/C-9 Dtsd), 26.3 (CH<sub>2</sub>, C-7/C-9 Dtsd), 38.1 (CH<sub>2</sub>, C-3 Dtsd), 41.9 (CH<sub>2</sub>, C-6/C-10 Dtsd), 42.5 (CH<sub>2</sub>, C-6/C-10 Dtsd), 50.1 (2 CH<sub>2</sub>, C-3, C-5 Piperaz), 53.7 (2 CH<sub>2</sub>, C-2, C-6 Piperaz), 55.1 (CH<sub>3</sub>, OCH<sub>3</sub>), 55.2 (CH, C-2 Dtsd), 61.2 (CH<sub>2</sub>, CH<sub>2</sub>N), 69.3 (C, C-5 Dtsd), 111.0 (CH, C-3 Arom), 117.8 (CH, C-5 Arom), 120.6 (CH, C-6 Arom), 122.6 (CH, C-4 Arom), 141.0 (C, C-1 Arom), 151.9 (C, C-2 Arom).

The free amine (0.136 g, 0.36 mmol) was dissolved in Et<sub>2</sub>O and treated with 1.2 eq. of oxalic acid to give 0.128 g (0.27 mmol, 76% yield) of the corresponding oxalate salt.

Mp: 170–172 °C. <sup>1</sup>H NMR (600 MHz, DMSO-*d*<sub>6</sub>) δ 1.31–1.43 (m, 2H, CH<sub>2</sub>-8 Dtsd), 1.48–1.66 (m, 4H, CH<sub>2</sub>-7, CH<sub>2</sub>-9 Dtsd), 1.86–2.07 (m, 4H, CH<sub>2</sub>-6, CH<sub>2</sub>-10 Dtsd), 2.64–3.42 (m, 12H, CH<sub>2</sub>-2, CH<sub>2</sub>-3, CH<sub>2</sub>-5, CH<sub>2</sub>-6 Piperaz, CH<sub>2</sub>N, CH<sub>2</sub>-3 Dtsd), 3.78 (s, 3H, OCH<sub>3</sub>), 4.09 (m, 1H, CH-2 Dtsd), 6.83–7.03 (m, 4H, Arom). HRMS-ESI *m/z* [M+H]<sup>+</sup> calcd for C<sub>20</sub>H<sub>31</sub>N<sub>2</sub>O<sub>5</sub>S<sub>2</sub><sup>+</sup>: 379.1872; found 379.1872. Anal. calcd for C<sub>22</sub>H<sub>32</sub>N<sub>2</sub>O<sub>5</sub>S<sub>2</sub>: C 56.38, H 6.88, N 5.98; found: C 56.48, H 7.02, N 6.11.

#### 4.6.7. {1,4-Dithiaspiro[4.5]decan-2-ylmethyl}(2-phenoxyethyl)amine (**14**)

The title compound was purified by flash chromatography on silica gel cartridge (70/30 Cy/EtAc) to afford 0.032 g (0.1 mmol, 15%) of **14** as yellow oil.

<sup>1</sup>H NMR (400 MHz, CDCl<sub>3</sub>) δ 1.18–1.49 (m, 6H, CH<sub>2</sub>-7, CH<sub>2</sub>-8, CH<sub>2</sub>-9 Dtsd), 1.64 (m, 4H, CH<sub>2</sub>-6, CH<sub>2</sub>-10 Dtsd), 2.95 (dd, *J* = 7.4, 12.2 Hz, 1H, CHaNH), 3.02 (dd, *J* = 6.9, 12.2 Hz, 1H, CHbNH), 3.05 (t, *J* = 5.2 Hz, 2H, NHCH<sub>2</sub>CH<sub>2</sub>), 3.19 (dd, *J* = 5.6, 12.0 Hz, 1H, CHa-3 Dtsd), 3.35 (dd, *J* = 12.0, 5.1 Hz, 1H, CHb-3 Dtsd), 3.83–3.95 (m, 1H, CH-2 Dtsd), 4.08 (t, *J* = 5.3 Hz, 2H, CH<sub>2</sub>O), 6.81–7.08 (m, 3H, CH-2, CH-4, CH-6 Ph), 7.21–7.39 (m, 2H, CH-3, CH-5 Ph). <sup>13</sup>C NMR (100 MHz, CDCl<sub>3</sub>): δ 24.3 (CH<sub>2</sub>, C-8 Dtsd), 24.9 (CH<sub>2</sub>, C-7/C-9 Dtsd), 25.1 (CH<sub>2</sub>, C-7/C-9 Dtsd), 38.4 (CH<sub>2</sub>, C-3 Dtsd), 40.9 (CH<sub>2</sub>, C-6/C-10 Dtsd), 41.6 (CH<sub>2</sub>, C-6/C-10 Dtsd), 48.4 (CH<sub>2</sub>, NCH<sub>2</sub>CH<sub>2</sub>), 50.5 (CH, C-2 Dtsd), 52.4 (CH<sub>2</sub>, CHCH<sub>2</sub>N), 68.2 (CH<sub>2</sub>, CH<sub>2</sub>O), 69.0 (C, C-5 Dtsd), 114.2 (2 CH, C-2, C-6 Ph), 120.7 (CH, C-4 Ph), 129.2 (2 CH, C-3, C-5 Ph), 158.6 (C, C-1 Ph).

The free amine (0.032 g, 0.099 mmol) was dissolved in acetone and treated with 1.2 eq. of oxalic acid to give 0.038 g (0.092 mmol, 92% yield) of the corresponding oxalate salt.

Mp: 211–214 °C. <sup>1</sup>H NMR (600 MHz, DMSO-*d*<sub>6</sub>) δ 1.34–1.41 (m, 2H, CH<sub>2</sub>-8 Dtsd), 1.50–1.65 (m, 4H, CH<sub>2</sub>-7, CH<sub>2</sub>-9 Dtsd), 1.89–2.02

(m, 4H, CH<sub>2</sub>-6, CH<sub>2</sub>-10 Dtsd), 3.16 (dd, *J* = 5.3, 12.3 Hz, 1H, CHa-3 Dtsd), 3.27–3.45 (m, 5H, CH<sub>2</sub>N, CH<sub>2</sub>CH<sub>2</sub>O, CHb-3 Dtsd), 4.07 (m, 1H, CH-2 Dtsd), 4.20 (t, *J* = 5.2 Hz, 2H, CH<sub>2</sub>O), 6.93–7.01 (m, 3H, CH-2, CH-4, CH-6 Ph), 7.21–7.33 (m, 2H, CH-3, CH-5 Ph). HRMS-ESI *m/z* [M+H]<sup>+</sup> calcd for C<sub>17</sub>H<sub>26</sub>NOS<sub>2</sub><sup>+</sup>: 324.1449; found 324.1450. Anal. calcd for C<sub>19</sub>H<sub>27</sub>NO<sub>5</sub>S<sub>2</sub>: C 55.18, H 6.58, N 3.39; found: C 55.33, H 6.71, N 3.57.

#### 4.6.8. {1,4-Dithiaspiro[4.5]decan-2-ylmethyl}[2-(2-methoxyphenoxy)ethyl]amine (**15**)

The title compound was purified by flash chromatography on silica gel cartridge (50/50 Cy/EtAc) to afford 0.183 g (0.52 mmol, 47%) of **15** as dark oil.

<sup>1</sup>H NMR (400 MHz, CDCl<sub>3</sub>) δ 1.21–1.40 (m, 2H, CH<sub>2</sub>-8 Dtsd), 1.49–1.69 (m, 4H, CH<sub>2</sub>-7, CH<sub>2</sub>-9 Dtsd), 1.83–2.14 (m, 4H, CH<sub>2</sub>-6, CH<sub>2</sub>-10 Dtsd), 2.89 (dd, *J* = 7.0, 12.1 Hz, 1H, CHaNH), 2.93–3.16 (m, 3H, CHaNH, NHCH<sub>2</sub>CH<sub>2</sub>), 3.19 (dd, *J* = 5.7, 12.0 Hz, 1H, CHa-3 Dtsd), 3.35 (dd, *J* = 5.1, 12.0 Hz, 1H, CHb-3 Dtsd), 3.81–3.92 (m, 4H, OCH<sub>3</sub>, CH-2 Dtsd), 4.16 (t, *J* = 5.3 Hz, 2H, CH<sub>2</sub>O), 6.73–7.06 (m, 4H, Ph). <sup>13</sup>C NMR (100 MHz, CDCl<sub>3</sub>): δ 24.2 (CH<sub>2</sub>, C-8 Dtsd), 24.8 (CH<sub>2</sub>, C-7/C-9 Dtsd), 25.4 (CH<sub>2</sub>, C-7/C-9 Dtsd), 37.9 (CH<sub>2</sub>, C-3 Dtsd), 40.8 (CH<sub>2</sub>, C-6/C-10 Dtsd), 41.4 (CH<sub>2</sub>, C-6/C-10 Dtsd), 48.5 (CH<sub>2</sub>, NCH<sub>2</sub>CH<sub>2</sub>), 50.3 (CH, C-2 Dtsd), 52.5 (CH<sub>2</sub>, CHCH<sub>2</sub>N), 55.8 (CH<sub>3</sub>, OCH<sub>3</sub>), 68.6 (CH<sub>2</sub>, CH<sub>2</sub>O), 69.0 (C, C-5 Dtsd), 111.9 (CH, C-3 Ph), 114.3 (CH, C-5 Ph), 120.8 (CH, C-6 Ph), 121.5 (CH, C-4 Ph), 147.9 (C, C-1 Ph), 149.7 (C, C-2 Ph).

The free amine (0.183 g, 0.52 mmol) was dissolved in Et<sub>2</sub>O and treated with 1.2 eq. of oxalic acid to give 0.216 g (0.486 mmol, 94% yield) of the corresponding oxalate salt.

Mp: 206–207 °C. <sup>1</sup>H NMR (600 MHz, DMSO-*d*<sub>6</sub>) δ 1.34–1.44 (m, 2H, CH<sub>2</sub>-8 Dtsd), 1.48–1.65 (m, 4H, CH<sub>2</sub>-7, CH<sub>2</sub>-9 Dtsd), 1.86–2.01 (m, 4H, CH<sub>2</sub>-6, CH<sub>2</sub>-10 Dtsd), 3.18 (dd, *J* = 5.1, 12.5 Hz, 1H, CHa-3 Dtsd), 3.30–3.44 (m, 5H, CH<sub>2</sub>N, CH<sub>2</sub>CH<sub>2</sub>O, CHb-3 Dtsd), 3.78 (s, 3H, OCH<sub>3</sub>), 4.11 (m, 1H, CH-2 Dtsd), 4.21 (t, *J* = 5.4 Hz, 2H, CH<sub>2</sub>O), 6.86–7.04 (m, 4H, Ph). HRMS-ESI *m/z* [M+H]<sup>+</sup> calcd for C<sub>18</sub>H<sub>28</sub>NO<sub>6</sub>S<sub>2</sub><sup>+</sup>: 354.116; found 354.1556. Anal. calcd for C<sub>20</sub>H<sub>29</sub>NO<sub>6</sub>S<sub>2</sub>: C 54.15, H 6.59, N 3.16; found: C 54.17, H 6.762, N 3.19.

### 4.7. Biological assays

#### 4.7.1. Radioligand binding assay at human recombinant 5-HT<sub>1A</sub>R and α<sub>1</sub> adrenoceptor subtypes

A human cell line (HeLa) stably transfected with genomic clone G-21 coding for the human 5-HT<sub>1A</sub> serotonergic receptor was used. Cells were grown as monolayers in Dulbecco's modified Eagle's medium supplemented with 10% fetal calf serum and gentamycin (100 µg/mL) under 5% CO<sub>2</sub> at 37 °C. Cells were detached from the growth flask at 95% confluence by a cell scraper and were lysed in ice-cold Tris (5 mM) and EDTA buffer (5 mM, pH 7.4). Homogenates were centrifuged for 20 min at 40000 g, and pellets were resuspended in a small volume of ice-cold Tris/EDTA buffer (above) and immediately frozen and stored at 70 °C until use. On the day of experiment, cell membranes (80–90 µg of protein) were resuspended in binding buffer (50 mM Tris, 2.5 mM MgCl<sub>2</sub>, and 10 mM pargiline, pH 7.4). Membranes were incubated in a final volume of 0.32 mL for 30 min at 30 °C with 1 nM [<sup>3</sup>H]8-OH-DPAT, in the absence or presence of various concentrations of the competing drugs (1 pM–1 µM); each experimental condition was performed in triplicate. Nonspecific binding was determined in the presence of 10 µM 5-HT [42]. Binding to recombinant human α<alpha>1 adrenoceptor subtypes was performed in membranes from Chinese hamster ovary (CHO) cells transfected by electroporation with DNA expressing the gene encoding each α1 adrenoceptor subtype. Cloning and stable expression of the human α1 adrenoceptor genes were performed as described [41]. CHO cell membranes (70 µg of

protein) were incubated in 50 mM Tris (pH 7.4) with 0.1–0.4 nM [ $^3\text{H}$ ]prazosin, in a final volume of 0.32 mL for 30 min at 25 °C, in the absence or presence of competing drugs (1 pM–1  $\mu\text{M}$ ). Nonspecific binding was determined in the presence of 10  $\mu\text{M}$  Tamsulosin. The incubation was stopped by addition of ice-cold Tris buffer and rapid filtration through Unifilter B filters (Perkin-Elmer) using a Filtermate cell harvester (Packard), and the radioactivity retained on the filters was determined by TopCount, Perkin-Elmer liquid scintillation counting at 90% efficiency.

#### 4.7.2. [ $^{35}\text{S}$ ]GTP $\gamma\text{S}$ binding assay

The effects of the various compounds tested on [ $^{35}\text{S}$ ]GTP $\gamma\text{S}$  binding in HeLa cells expressing the recombinant human 5-HT $_{1A}$  receptor were evaluated according to the method of Stanton and Beer [43] with minor modifications [44,52]. Stimulation experiments: Cell membranes (50–70  $\mu\text{g}$  of protein) were resuspended in buffer containing 20 mM HEPES, 3 mM MgSO $_4$ , and 120 mM NaCl (pH 7.4). The membranes were incubated with 30  $\mu\text{M}$  GDP, and various concentrations (from 0.01 nM to 10  $\mu\text{M}$ ) of test drugs or 8-OH-DPAT (reference curve) for 20 min at 30 °C in a final volume of 0.5 mL. Samples were transferred to ice, [ $^{35}\text{S}$ ]GTP $\gamma\text{S}$  (200 pM) was added, and samples were incubated for another 30 min at 30 °C. The pre-incubation with both agonist and antagonist, before initiating the [ $^{35}\text{S}$ ]GTP $\gamma\text{S}$  binding, ensures that agonist and antagonist are at equilibrium. Nonspecific binding was determined in the presence of 10  $\mu\text{M}$  GTP $\gamma\text{S}$ . Incubation was stopped by the addition of ice-cold HEPES buffer and rapid filtration on Unifilter B filters (Perkin Elmer) using a Filtermate cell harvester (Packard). The filters were washed with ice-cold Hepes buffer, and the radioactivity retained on the filters was determined by TopCount, Perkin Elmer liquid scintillation counting at 90% efficiency.

#### 4.8. Data analysis

Binding data were analyzed using the nonlinear curve-fitting program GraphPad (Prism for windows, version 5.04). Scatchard plots were linear for all preparations. None of the pseudo-Hill coefficients (nH) were significantly different from unity ( $p > 0.05$ ). Equilibrium dissociation constants ( $K_i$ ) were derived from the Cheng–Prusoff equation  $K_i = \text{IC}_{50}/(L/K_d)$ , where L and  $K_d$  are the concentration and the equilibrium dissociation constant of the radioligand.  $\text{p}K_i$  values are the mean of 2–3 separate experiments performed in duplicate [61]. Stimulation of [ $^{35}\text{S}$ ]GTP $\gamma\text{S}$  binding induced by the compounds tested was expressed as the percent increase in binding above basal value, with the maximal stimulation observed with 8-OH-DPAT taken as 100%. The concentration–response curves of the agonistic activity were analyzed by GraphPad as reported above [62]. The maximum percentage of stimulation of [ $^{35}\text{S}$ ]GTP $\gamma\text{S}$  binding ( $E_{\text{max}}$ ) achieved for each drug, and the concentration required to obtain 50% of  $E_{\text{max}}$  ( $\text{pD}_2 = -\log_{10}[\text{EC}_{50}]$ ), were evaluated.

#### 4.9. Cytotoxicity assays

Cytotoxicity assays were carried out against human neuroblastoma cell line SH-SY5Y. Cells were cultured at 37 °C in a humidified incubator containing 5% CO $_2$  and feed with DMEM (Lonza) nutrient supplemented with 10% heat inactivated FBS, 2 mM L-glutamine, 100 U/mL penicillin and 100  $\mu\text{g}/\text{mL}$  streptomycin. Cytotoxicity of compounds is expressed as IC $_{50}$  values, the concentrations that cause 50% growth inhibition. The results were determined using the 3-(4,5-dimethylthiazol-2-yl)-2,5-diphenyl-tetrazolium bromide [51]. Cells were dispensed into 96-well microtiter plates at a density of 10,000 cells/well. Following overnight incubation, cells were treated with the tested compounds, oligomycin A and

rotenone in the range concentration 0.1–100  $\mu\text{M}$ , and with the range 1–500  $\mu\text{M}$  for H $_2\text{O}_2$ . Then the plates were incubated at 37 °C for 24 h. An amount of 10  $\mu\text{L}$  of 0.5% w/v MTT was further added to each well and the plates were incubated for an additional 3 h at 37 °C. Finally the cells were lysed by addition of 100  $\mu\text{L}$  of DMSO/EtOH 1:1 (v/v) solution. The absorbance at 570 nm was determined using a Perkin Elmer 2030 multilabel reader Victor TM X3.

#### 4.10. Neuroprotective capacity

The neuroprotective capacity of the compounds was tested, as reported by Benchekroun et al. [45] Briefly, the ability of the compounds to prevent the human neuroblastoma cell line SH-SY5Y from death was evaluated by using three toxicity models: 1) H $_2\text{O}_2$ , as a producer of exogenous free radicals, 2) oligomycin A, a mitochondrial respiratory chain blocker which produces mitochondrial ROS by inhibiting the mitochondrial electron-transport chain complex V, and 3) rotenone, showing the same effect of oligomycin A by inhibiting the mitochondrial electron-transport chain complex I. In this experiment, the toxic insults were used at the concentrations equal to their IC $_{50}$  after 24 h of incubation: 195, 30 and 75  $\mu\text{M}$  for H $_2\text{O}_2$ , oligomycin A and rotenone, respectively. The tested compounds were used at non-cytotoxic concentrations after 24 h of incubation. Compounds that are able of inhibiting the effect of the toxic insults may be considered neuroprotectants [63]. For the assay, SH-SY5Y cells were plated in 96-well plates at a seeding density of 10,000 cells/well. After 24 h of incubation at 37 °C in a humidified incubator containing 5% CO $_2$ , cells were co-incubated with H $_2\text{O}_2$  (195  $\mu\text{M}$ ), or oligomycin A (30  $\mu\text{M}$ ), or rotenone (75  $\mu\text{M}$ ) and tested compound at several concentration for further 24 h. In particular, compound **15** was tested at concentrations 0.1 and 1  $\mu\text{M}$ . The cell viability was determined by MTT assay and analyzed as previously described.

#### 4.11. Bi-directional transport studies on MDCKII-MDR1 monolayers

Apical to basolateral (Papp, AP) and basolateral to apical (Papp, BL) permeability of the tested compounds was measured using Madin-Darby Canine Kidney (i.e., MDCK) cells, retrovirally transfected with the human MDR1 cDNA (MDCKII-MDR1), as previously reported [49,50]. The cells were cultured in DMEM medium and seeded at a density of 100,000 cell/cm $^2$  onto polyester 12 well Transwell inserts (pore size 0.4  $\mu\text{m}$ , 12 mm diameter, apical volume 0.5 mL, basolateral volume 1.5 mL). At first, MDCKII-MDR1 cell barrier function was verified by means of *trans*-epithelial electrical resistance (TEER) using an EVOM apparatus and by the measurement of the flux of the paracellular standard fluorescein isothiocyanate-dextran (FD4, Sigma) (200  $\mu\text{g}/\text{mL}$ ) and the trans-cellular standard diazepam (75  $\mu\text{M}$ ). The TEER was measured in growth media at room temperature and calculated as the measured resistance minus the resistance of an empty Transwell (blank without cells). Cell monolayers with TEER values 800 Ohm cm $^2$  were used for the successive transport experiments. The cells were equilibrated in transport medium in both the apical and basolateral chambers for 30 min at 37 °C. The composition of transport medium was: 0.4 mM K $_2\text{HPO}_4$ , 25 mM NaHCO $_3$ , 3 mM KCl, 122 mM NaCl, 10 mM glucose with final pH of 7.4, and the osmolarity was 300 mOsm as determined by a freeze point based osmometer. At time 0, culture medium was aspirated from both the apical (AP) and basolateral (BL) chambers of each insert, and cell monolayers were washed three times (10 min per wash) with Dulbecco's Phosphate Buffered Saline (DPBS) pH = 7.4. Finally, a solution of compounds diluted in transport medium was added to the apical or basolateral chamber. For AP-to-BL or BL-to-AP flux studies, the drug solution was added in the AP chamber or in the BL chamber, respectively.

Except for FD4, which was solubilized directly in the assay medium at a concentration of 200 µg/mL, the other compounds were first dissolved in DMSO and then diluted with the assay medium to a final concentration of 75 µM. Next, the tested solutions were added to the donor side (0.5 mL for the AP chamber and 1.5 mL for the BL chamber) and fresh assay medium was placed in the receiver compartment. The percentage of DMSO never exceeded 1% (v/v) in the samples. The transport experiments were carried out under cell culture conditions (37 °C, 5% CO<sub>2</sub>, 95% humidity). After incubation time of 120 min, samples were removed from the apical and basolateral side of the monolayer and then stored until further analysis. Quantitative analysis of the tested compounds and diazepam, was performed through UV–visible (Vis) spectroscopy using a PerkinElmer double-beam UV–visible spectrophotometer Lambda Bio 20 (Milan, Italy), equipped with 10 mm path-length-matched quartz cells. Standard calibration curves were prepared at maximum absorption wavelength of each compound using PBS as solvent and were linear ( $r^2 = 0.999$ ) over the range of tested concentration (from 5 to 100 µM). The FD4 samples were analyzed with a Victor3 fluorometer (Wallac Victor3, 1420 Multilabel Counter, Perkin-Elmer) at excitation and emission wavelengths of 485 and 535 nm, respectively. Each compound was tested in triplicate, and the experiments were repeated three times.

The apparent permeability, in units of cm/sec, was calculated using the following equation:

$$P_{\text{app}} = \left( \frac{V_A}{\text{area} \times \text{time}} \right) \times \left( \frac{[\text{drug}]_{\text{acceptor}}}{[\text{drug}]_{\text{initial}}} \right)$$

where “VA” is the volume in the acceptor well, “area” is the surface area of the membrane, “time” is the total transport time, “[drug]<sub>acceptor</sub>” is the concentration of the drug measured by UV-spectroscopy and “[drug]<sub>initial</sub>” is the initial drug concentration in the AP or BL chamber. Efflux ratio (ER) was calculated using the following equation: ER = P<sub>app, BL-AP</sub>/P<sub>app, AP-BL</sub>, where P<sub>app, BL-AP</sub> is the apparent permeability of basal-to-apical transport, and P<sub>app, AP-BL</sub> is the apparent permeability of apical-to-basal transport. An efflux ratio greater than 2 indicates that a test compound is likely to be a substrate for P-gp transport.

#### 4.12. Antinociceptive activity in in-vivo model

For the assessment of antinociceptive activity of inflammatory pain, mice were subjected to the formalin test. Male Swiss CB1 mice (Envigo, S.Pietro al Natisone (UD)) weighing 25–30 g were used. Animals were kept at a constant room temperature (25 ± 1 °C) under a 12:12 h light and dark cycle with free access to food and water. Each mouse was used for only one experiment. Experimental procedures were approved by the Local Ethical Committee (IACUC) and conducted in accordance with international guidelines as well as European Communities Council Directive and National Regulations (CEE Council 86/609 and DL 116/92). All tests were performed blind to treatment.

Formalin (5%, 10 µl; Sigma-Aldrich) was injected subcutaneously into the plantar side of the right hind paw [64]. After the injection, mice were immediately placed in a plexiglas box: the total time (in seconds) spent on licking or biting the injected hind paw was recorded for each 5 min in selected intervals, 0–10 (phase I) and 10–60 (phase II) min, in the different experimental group as indicator of nociceptive behavior. Formalin scores were separated in two phases: phase I (0–10 min) and phase II (10–60 min). A mean response was then calculated for each phase. Compound **15** and WAY-100635 (Sigma-Aldrich) were dissolved in normal saline solution containing 10% dimethyl sulfoxide (DMSO, Sigma-Aldrich). A

vehicle solution containing 10% DMSO was given as control. Compound **15** and vehicle were intraplantar (i.p.) administered (5 ml/kg) 15 min before formalin. WAY-100635 (3 mg/kg i.p.) was injected 30 min before test compound or vehicle. Data are expressed as mean values (SEM). Analysis of variance (two-way repeated measures ANOVA followed by post hoc Bonferroni test) were performed to assess significance using the InStat 3.0 software (GraphPad Software, San Diego, CA).  $p < 0.05$  was considered significant.

## 5. Molecular modeling

### 5.1. Ligand preparation

Compounds **A** and **9–11**, **14–16**, **19–21** were built, parameterised (Gasteiger-Huckel method) and energy minimized within MOE using MMFF94 force field [65]. For all compounds, the protonated form was considered for the *in silico* analyses.

### 5.2. Alpha<sub>1D</sub> homology modeling

The alpha<sub>1D</sub> theoretical model has been built starting from the X-ray structure of the β<sub>2</sub>-adrenoreceptor (PDB code: 2RH1; resolution = 2.40 Å) [66], by applying the ligand-based homology modeling strategy. In particular, compound **A** was docked into the β<sub>2</sub>-adrenoreceptor binding site and employed in the alpha<sub>1D</sub> model building and refinement, by taking into account the ligand specific steric and chemical features. The amino acid sequence of α<sub>1D</sub>-adrenoreceptor (P25100) was retrieved from the SWISSPROT database [67] while the three-dimensional structure co-ordinates file of the GPCR template was obtained from the Protein Data Bank [68]. The amino acid sequences of α<sub>1D</sub> TM helices were aligned with the corresponding residues of 2RH1, on the basis of the Blosum62 matrix (MOE software). The connecting loops were constructed by the loop search method implemented in MOE. The MOE output file included a series of ten models which were independently built on the basis of a Boltzmann-weighted randomized procedure [69], combined with specialized logic for the handling of sequence insertions and deletions [70]. Among the derived models, there were no significant main chain deviations. The model with the best packing quality function was selected for full energy minimization. The retained structure was minimized with MOE using the AMBER94 force field [71]. The energy minimization was carried out by the 1000 steps of steepest descent followed by conjugate gradient minimization until the rms gradient of the potential energy was less than 0.1 kcal mol<sup>-1</sup> Å<sup>-1</sup>. The assessment of the final obtained model was performed using Ramachandran plots, generated within MOE.

### 5.3. Docking studies

Docking studies were performed according to the following protocol. The binding site of the ligand in the 5HT<sub>1A</sub> receptor model (previously built by us) was determined starting from the fact that, for the ligand activity, formation of the salt bridge between the protonated piperazine nitrogen on the ligand and Asp116 is necessary [72–74].

On the other hand, the α<sub>1D</sub>-adrenoreceptor binding site has been determined taking into account the conserved residues highlighted by superimposition on the 2RH1 X-ray β<sub>2</sub>-adrenoreceptor binding site. For all compounds, each isomer was docked into the putative ligand binding site by means of the Surflex docking module implemented in Sybyl-X1.0 [75].

Surflex-Dock uses an empirically derived scoring function based on the binding affinities of X-ray protein-ligand complexes. The Surflex-Dock scoring function is a weighted sum of non-linear



functions involving van der Waals surface distances between the appropriate pairs of exposed protein and ligand atoms, including hydrophobic, polar, repulsive, entropic and solvation and crash terms represented in terms of a total score conferred to any calculated conformer.

Then, for all compounds, the best docking geometries (selected on the basis of the SurFlex scoring functions) were refined by ligand/receptor complex energy minimization (CHARMM27) by means of the MOE software. To verify the reliability of the derived docking poses, the obtained ligand/receptor complexes were further investigated by docking calculations (10 run), using MOE-Dock (Genetic algorithm; applied on the poses already located into the putative 5-HT<sub>1A</sub> and alpha<sub>1D</sub> receptors). The conformers showing lower energy scoring functions and rmsd values (respect to the starting poses) were selected as the most stable and allowed us to identify the most probable conformers interacting with the two GPCRs.

#### 5.4. Prediction of ADMET properties

The prediction of ADMET properties were performed using the Advanced Chemistry Development (ACD) Percepta platform. The aforementioned descriptors blood-brain barrier permeation (LogBBB), rate of passive diffusion-permeability (Log PS), human intestinal absorption (HIA), volume of distribution (Vd), median lethal dose (LD<sub>50</sub>) related to oral administration and the logarithmic ratio of the octanol-water partitioning coefficient (cLogP) were calculated. All of them were derived and evaluated by Percepta on the basis of training libraries, implemented in the software, which include a consistent number of molecules whose pharmacokinetic and toxicity profile are known.

#### Acknowledgment

The authors thank Ms. Rossella Gallesi for performing the elemental analysis.

#### Appendix A. Supplementary data

Supplementary data related to this article can be found at <http://dx.doi.org/10.1016/j.ejmech.2016.09.050>.

#### References

- [1] J. Hannon, D. Hoyer, Molecular biology of 5-HT receptors, *Behav. Brain Res.* 195 (2008) 198–213.
- [2] D.E. Nichols, C.D. Nichols, Serotonin receptors, *Chem. Rev.* 108 (2008) 1614–1641.
- [3] A. Fargin, J.R. Raymond, M.J. Lohse, B.K. Kobilka, M.G. Caron, R.J. Lefkowitz, The genomic clone G-21 which resembles a  $\beta$ -adrenergic-receptor sequence encodes the 5-HT<sub>1A</sub> receptor, *Nature* 335 (1988) 358–360.
- [4] F. Fiorino, B. Severino, F. Magli, A. Ciano, G. Caliendo, V. Santagada, F. Frecentese, E. Perissutti, 5-HT<sub>1A</sub> receptor: an old target as a new attractive tool in drug discovery from central nervous system to Cancer, *J. Med. Chem.* 57 (2014) 4407–4426.
- [5] R. Schreiber, J. De Vry, 5-HT<sub>1A</sub> receptor ligands in animal models of anxiety, impulsivity and depression: multiple mechanisms of action? *Prog. Neuro-Psychopharmacol. Biol. Psychiatry* 17 (1993) 87–104.
- [6] P. Blier, N.M. Ward, Is there a role for 5-HT<sub>1A</sub> agonists in the treatment of depression? *Biol. Psychiatry* 53 (2003) 193–203.
- [7] M. Delgado, A.G. Caicoya, V. Greciano, B. Benhamu, M.L. Lopez-Rodriguez, M.S. Fernandez-Alfonso, M.A. Pozo, J. Manzanares, J.A. Fuentes, Anxiolytic-like effect of a serotonergic ligand with high affinity for 5-HT<sub>1A</sub>, 5-HT<sub>2A</sub> and 5-HT<sub>3</sub> receptors, *Eur. J. Pharmacol.* 511 (2005) 9–19.
- [8] A.C. McCreary, C.A. Jones, Antipsychotic medication: the potential role of 5-HT<sub>1A</sub> receptor agonism, *Curr. Pharm. Des.* 16 (2010) 516–521.
- [9] Z. Liu, H. Zhang, N. Ye, J. Zhang, Q. Wu, P. Sun, L. Li, X. Zhen, A. Zhang, Synthesis of dihydrofuroaporphine derivatives: identification of a potent and selective serotonin 5-HT<sub>1A</sub> receptor agonist, *J. Med. Chem.* 53 (2010) 1319–1328.
- [10] L. Madhavan, W.J. Freed, V. Anantharam, A.G. Kanthasamy, 5-Hydroxytryptamine 1A receptor activation protects against N-methyl-D-aspartate-induced apoptotic cell death in striatal and mesencephalic cultures, *J. Pharmacol. Exp. Ther.* 304 (2003) 913–923.
- [11] A.C. Berends, P.G. Luiten, C. Nyakas, A review of the neuroprotective properties of the 5-HT<sub>1A</sub> receptor agonist rebinotan HCl (BAYx3702) in ischemic stroke, *CNS Drug Rev.* 11 (2005) 379–402.
- [12] C.P. Chang, S.H. Chen, M.T. Lin, Ipsapirone and ketanserin protects against circulatory shock, intracranial hypertension, and cerebral ischemia during heatstroke, *Shock* 24 (2005) 336–340.
- [13] N.P. Iannuzzi, D.S. Liebeskind, M. Jacoby, K. Arima, K. Shimizu, D. Asubio, T.R. Zimmerman, Piclozotan (SUN N4057), a novel 5-HT<sub>1A</sub> receptor agonist, is well tolerated in patients with acute stroke, *Stroke* 37 (2006) 655, 655.
- [14] K. Kamei, N. Maeda, K. Nomura, M. Shibata, R. Katsuragi-Ogino, M. Koyama, M. Nakajima, T. Inoue, T. Ohno, T. Tatsuoka, Synthesis, SAR studies, and evaluation of 1,4-benzoxazepine derivatives as selective 5-HT<sub>1A</sub> receptor agonists with neuroprotective effect: discovery of piclozotan, *Bioorg. Med. Chem.* 14 (2006) 1978–1992.
- [15] P. Teal, S. Davis, W. Hacke, M. Kaste, P.D. Lyden, M. Fierus, A randomized, double-blind, placebo-controlled trial to evaluate the efficacy, safety, tolerability, and pharmacokinetic/pharmacodynamic effects of a targeted exposure of intravenous rebinotan in patients with acute ischemic stroke modified randomized exposure controlled trial, *Stroke* 40 (2009) 3518–3525.
- [16] I. Marco, M. Valhondo, M. Martin-Fontecha, H. Vazquez-Villa, J. Del Rio, A. Planas, O. Sagredo, J.A. Ramos, I.R. Torrecillas, L. Pardo, D. Frechilla, B. Benhamu, M.L. Lopez-Rodriguez, New serotonin 5-HT<sub>1A</sub> receptor agonists with neuroprotective effect against ischemic cell damage, *J. Med. Chem.* 54 (2011) 7986–7999.
- [17] N. Nakata, H. Suda, J. Izumi, Y. Tanaka, Y. Ikeda, H. Kato, Y. Itoyama, K. Kogure, Role of hippocampal serotonergic neurons in ischemic neuronal death, *Behav. Brain Res.* 83 (1997) 217–220.
- [18] B.J. Oosterink, S. Korte, C. Nyakas, J. Korf, P.G. Luiten, Neuroprotection against N-methyl-D-aspartate-induced excitotoxicity in rat magnocellular nucleus basalis by the 5-HT<sub>1A</sub> receptor agonist 8-OH-DPAT, *Eur. J. Pharmacol.* 358 (1998) 147–152.
- [19] D.B. Carr, D.C. Cooper, S.L. Ulrich, N. Spruston, D.J. Surmeier, Serotonin receptor activation inhibits sodium current and dendritic excitability in prefrontal cortex via a protein kinase C-dependent mechanism, *J. Neurosci.* 22 (2002) 6846–6855.
- [20] S. Namura, J. Zhu, K. Fink, M. Endres, A. Srinivasan, K.J. Tomaselli, J. Yuan, M.A. Moskowitz, Activation and cleavage of caspase-3 in apoptosis induced by experimental cerebral ischemia, *J. Neurosci.* 18 (1998) 3659–3668.
- [21] D. Galter, K. Unsicker, Sequential activation of the 5-HT<sub>1A</sub> serotonin receptor and TrkB induces the serotonergic neuronal phenotype, *Mol. Cell. Neurosci.* 15 (2000) 446–455.
- [22] P. Calabresi, M. Di Filippo, V. Ghiglieri, B. Picconi, Molecular mechanisms underlying levodopa-induced dyskinesia, *Mov. Disord.* 23 (2008) S570–S579.
- [23] E. Calcagno, M. Carli, R.W. Invernizzi, The 5-HT<sub>1A</sub> receptor agonist 8-OH-DPAT prevents prefrontocortical glutamate and serotonin release in response to blockade of cortical NMDA receptors, *J. Neurochem.* 96 (2006) 853–860.
- [24] M. Carta, T. Carlsson, A. Munoz, D. Kirik, A. Bjorklund, Serotonin–dopamine interaction in the induction and maintenance of L-DOPA-induced dyskinesias, *Prog. Brain Res.* 172 (2008) 465–478.
- [25] M.M. Irvani, K. Tayarani-Binazir, W.B. Chu, M.J. Jackson, P. Jenner, In 1-methyl-4-phenyl-1,2,3,6-tetrahydropyridine-treated primates, the selective 5-hydroxytryptamine 1A agonist (R)-(+)-8-OHDPAT inhibits levodopa-induced dyskinesia but only with increased motor disability, *J. Pharmacol. Exp. Ther.* 319 (2006) 1225–1234.
- [26] W. Bara-Jimenez, F. Bibbiani, M.J. Morris, T. Dimitrova, A. Sherzai, M.M. Mouradian, T.N. Chase, Effects of serotonin 5-HT<sub>1A</sub> agonist in advanced Parkinson's disease, *Mov. Disord.* 20 (2005) 932–936.
- [27] S.H. Fox, R. Chuang, J.M. Brotchie, Serotonin and Parkinson's disease: on movement, mood, and madness, *Mov. Disord.* 24 (2009) 1255–1266.
- [28] L. Gregoire, P. Samadi, J. Graham, P.J. Bedard, G.D. Bartoszyk, T. Di Paolo, Low doses of sarizotan reduce dyskinesias and maintain antiparkinsonian efficacy of L-Dopa in parkinsonian monkeys, *Parkinsonism Relat. Disord.* 15 (2009) 445–452.
- [29] M.B. Assie, L. Bardin, A.L. Auclair, E. Carilla-Durand, R. Depoortere, W. Koek, M.S. Kleven, F. Colpaert, B. Vacher, A. Newman-Tancredi, F15599, a highly selective post-synaptic 5-HT<sub>1A</sub> receptor agonist: in-vivo profile in behavioural models of antidepressant and serotonergic activity, *Int. J. Neuro-psychopharmacol.* 11 (2010) 1–14.
- [30] A. Munoz, Q. Li, F. Gardoni, E. Marcelllo, C. Qin, T. Carlsson, D. Kirik, M. Di Luca, A. Bjorklund, E. Bezard, M. Carta, Combined 5-HT<sub>1A</sub> and 5-HT<sub>1B</sub> receptor agonists for the treatment of L-DOPA-induced dyskinesia, *Brain* 131 (2008) 3380–3394.
- [31] E. Bezard, E. Tronci, E.Y. Pioli, Q. Li, G. Porras, A. Bjorklund, M. Carta, Study of the antidyskinetic effect of eltopazine in animal models of levodopa-induced dyskinesia, *Mov. Disord.* 28 (2013) 1088–1096.
- [32] C.G. Goetz, P. Damier, C. Hicking, E. Laska, T. Muller, C.W. Olanow, O. Rascol, H. Russ, Sarizotan as a treatment for dyskinesias in Parkinson's disease: a double-blind placebo-controlled trial, *Mov. Disord.* 22 (2007) 179–186.
- [33] R. Nadeson, C.S. Goodchild, Antinociceptive role of 5-HT<sub>1A</sub> receptors in rat spinal cord, *Br. J. Anaesth.* 88 (2002) 679–684.
- [34] J.A. Mico, E. Berrocoso, A. Ortega-Alvaro, J. Gibert-Rahola, M.O. Rojas-Corrales, The role of 5-HT<sub>1A</sub> receptors in research strategy for extensive pain treatment, *Curr. Top. Med. Chem.* 6 (2006) 1997–2003.

- [35] L. Björk, A. Fredriksson, U. Hacksell, T. Lewander, Effects of (R)-8-OH-DPAT and the enantiomers of UH-301 on motor activities in the rat: antagonism of (R)-8-OH-DPAT-induced effects, *Eur. Neuropsychopharmacol.* 2 (1992) 141–147.
- [36] V. Kayser, I.E. Elfassi, B. Aubel, M. Melfort, D. Julius, J.A. Gingrich, M. Hamon, S. Bourgoignie, Mechanical, thermal and formalin-induced nociception is differentially altered in 5-HT<sub>1A</sub><sup>-/-</sup>, 5-HT<sub>1B</sub><sup>-/-</sup>, 5-HT<sub>2A</sub><sup>-/-</sup>, 5-HT<sub>3A</sub><sup>-/-</sup> and 5-HT<sub>1</sub><sup>-/-</sup> knock-out male mice, *Pain* 130 (2007) 235–248.
- [37] M.L. Lopez-Rodríguez, D. Ayala, B. Benhamu, M.J. Morcillo, A. Viso, Arylpiperazine derivatives acting at 5-HT<sub>1A</sub> receptors, *Curr. Med. Chem.* 9 (2002) 443–446.
- [38] C. Sorbi, S. Franchini, A. Tait, A. Prandi, R. Gallesi, P. Angeli, G. Marucci, L. Pirona, E. Poggesi, L. Brasili, 1,3-Dioxolane-Based ligands as rigid analogues of naftopidil: structure–affinity/activity relationships at  $\alpha$ 1 and 5-HT<sub>1A</sub> receptors, *ChemMedChem* 4 (2009) 393–399.
- [39] S. Franchini, U.M. Battisti, A. Baraldi, A. Prandi, P. Fossa, E. Cichero, A. Tait, C. Sorbi, G. Marucci, A. Cilia, L. Pirona, L. Brasili, Structure–Affinity/Activity relationships of 1,4-dioxo-spiro[4.5]decane based ligands at  $\alpha$ 1 and 5-HT<sub>1A</sub> receptors, *Eur. J. Med. Chem.* 87 (2014) 248–266.
- [40] L. Brasili, C. Sorbi, S. Franchini, M. Manicardi, P. Angeli, G. Marucci, A. Leonardi, E. Poggesi, *J. Med. Chem.* 46 (2003) 1504–1511.
- [41] R. Testa, C. Taddei, E. Poggesi, C. Destefani, S. Cotecchia, J.P. Hieble, A.C. Sulpizio, D. Naselski, D. Bergsma, C. Ellis, A. Swift, S. Ganguli, R.R. Ruffolo, A. Leonardi, *Rec 15/2739 (SB 216469)* a novel prostate selective  $\alpha$ 1-adrenoceptor antagonist, *Pharmacol. Commun.* 6 (1995) 79–86.
- [42] R. Testa, L. Guarneri, E. Poggesi, P. Angelico, C. Velasco, M. Ibba, A. Cilia, G. Motta, C. Riva, A. Leonardi, Effect of several 5-Hydroxytryptamine 1A receptor ligands on the micturition reflex in rats: comparison with way 100635, *J. Pharmacol. Exp. Ther.* 290 (1999) 1258–1269.
- [43] J.A. Stanton, M.S. Beer, Characterisation of a cloned human 5-HT<sub>1A</sub> receptor cell line using [<sup>35</sup>S]GTP gamma S binding, *Eur. J. Pharmacol.* 320 (1997) 267–275.
- [44] S. Franchini, A. Prandi, C. Sorbi, A. Tait, A. Baraldi, P. Angeli, M. Buccioni, A. Cilia, E. Poggesi, P. Fossa, L. Brasili, Discovery of a new series of 5-HT<sub>1A</sub> receptor agonists, *Bioorg. Med. Chem. Lett.* 20 (2010) 2017–2021.
- [45] M. Benchekroun, M. Bartolini, J. Egea, A. Romero, E. Soriano, M. Pudlo, V. Luzet, V. Andrisano, M.L. Jimeno, M.G. López, S. Wehle, T. Gharbi, B. Refouvet, L. de Andrés, C. Herrera-Arozamena, B. Monti, M.L. Bolognesi, M.I. Rodríguez-Franco, M. Decker, J. Marco-Contelles, L. Ismaili, Novel tacrine-grafted ugi adducts as multipotent anti-Alzheimer drugs: a synthetic renewal in tacrine–ferulic acid hybrids, *ChemMedChem* 10 (2015) 523–539, <http://dx.doi.org/10.1002/cmcd.201402409>.
- [46] K. Vissers, H. Adriaensens, R. De Coster, C. De Deyne, T.F. Meert, A chronic-constriction injury of the sciatic nerve reduces bilaterally the responsiveness to formalin in rats: a behavioral and hormonal evaluation, *Anesth. Analg.* 97 (2003) 520–525.
- [47] R. Boehm, E. Hannig, Data on cyclic ketals. Part 8. Derivatization of 2,2-disubstituted 5-hydroxymethyl-1,3-oxathiolanes, *Pharmazie* 33 (1978) 27–29.
- [48] H. Waterbeemd, E. Gifford, ADMET in silico modelling: towards prediction paradise? *Nat. Rev. Drug Discov.* 2 (2003) 192–204.
- [49] N. Denora, V. Laquintana, A. Trapani, A. Lopodota, A. Latrofa, J.M. Gallo, G. Trapani, Translocator protein (TSPO) ligand-Ara-C (cytarabine) conjugates as a strategy to deliver antineoplastic drugs and to enhance drug clinical potential, *Mol. Pharm.* 7 (2010) 2255–2269.
- [50] N. Denora, T. Cassano, V. Laquintana, A. Lopalco, A. Trapani, C.S. Cimmino, L. Laconca, A. Giuffrida, G. Trapani, Novel codrugs with GABAergic activity for dopamine delivery in the brain, *Int. J. Pharm.* 437 (2012) 221–231.
- [51] N. Denora, V. Laquintana, A. Lopalco, R.M. Iacobazzi, A. Lopodota, A. Cutrignelli, G. Iacobellis, C. Annese, M. Cascione, S. Leporatti, M. Franco, In vitro targeting and imaging the translocator protein TSPO 18-kDa through G(4)-PAMAM-FITC labeled dendrimer, *J. Control. Release* 172 (2013) 1111–1125.
- [52] A. Prandi, S. Franchini, L. Ivanova Manasieva, P. Fossa, E. Cichero, G. Marucci, M. Buccioni, A. Cilia, L. Pirona, L. Brasili, Synthesis, biological evaluation, and docking studies of tetrahydrofuran- cyclopentanone- and cyclopentanol-based ligands acting at adrenergic  $\alpha$ 1- and serotonin 5-HT<sub>1A</sub> Receptors, *J. Med. Chem.* 55 (2012) 23–36.
- [53] S. Franchini, A. Prandi, A. Baraldi, C. Sorbi, A. Tait, M. Buccioni, G. Marucci, A. Cilia, L. Pirona, P. Fossa, E. Cichero, L. Brasili, 1,3-Dioxolane-based ligands incorporating a lactam or imide moiety: structure-affinity/activity relationship at  $\alpha$ 1-adrenoceptor subtypes and at 5-HT<sub>1A</sub> receptors, *Eur. J. Med. Chem.* 45 (2010) 3740–3751.
- [54] S. Moro, F. Deflorian, M. Bacilieri, G. Spalluto, Ligand-based homology modeling as attractive tool to inspect GPCR structural plasticity, *Curr. Pharm. Des.* 12 (2006) 2175–2185.
- [55] E. Cichero, P. D'Urso, M. Moscatelli, O. Bruno, A. Orro, C. Rotolo, L. Milanese, P. Fossa, Homology modeling, docking studies and molecular dynamic simulations using graphical processing unit architecture to probe the type-11 phosphodiesterase catalytic site: a computational approach for the rational design of selective inhibitors, *Chem. Biol. Drug Des.* 82 (2013) 718–731.
- [56] E. Cichero, S. Espinoza, R.R. Gainetdinov, L. Brasili, P. Fossa, Insights into the structure and pharmacology of the human trace amine-associated receptor 1 (hTAAR1): homology modelling and docking studies, *Chem. Biol. Drug Des.* 81 (2013) 509–516.
- [57] E. Cichero, G. Menozzi, S. Guariento, P. Fossa, Ligand-based homology modelling of the human CB2 receptor SR144528 antagonist binding site: a computational approach to explore the 1,5-diaryl pyrazole scaffold, *MedChemComm* 6 (2015) 1978–1986.
- [58] Y. Zheng, J. Wu, X. Feng, Y. Jia, J. Huang, Z. Hao, In silico analysis and experimental validation of lignan extracts from *Kadsura longipedunculata* for potential 5-HT<sub>1A</sub> agonists, *PLoS One* 10 (2015).
- [59] A.A. Kaczor, K.M. Targowska-Duda, B. Budzynska, B. Grazyna, A.G. Silva, M. Castro, In vitro, molecular modeling and behavioral studies of 3-[[4-(5-methoxy-1H-indol-3-yl)-1,2,3,6-tetrahydropyridin-1-yl]methyl]-1,2-dihydroquinolin-2-one (D2AAK1) as a potential antipsychotic, *Neurochem. Int.* 96 (2016).
- [60] A. Zagorska, M. Kotłaczkowski, A. Bucki, A. Siwek, G. Kazek, G. Satała, A.J. Bojarski, A. Partyka, A. Wesołowska, M. Pawłowski, Structure-activity relationships and molecular studies of novel arylpiperazinylalkyl purine-2,4-diones and purine-2,4,8-triones with antidepressant and anxiolytic-like activity, *Eur. J. Med. Chem.* 97 (2015) 142–154.
- [61] C. Yung-Chi, W.H. Prusoff, Relationship between the inhibition constant (K<sub>i</sub>) and the concentration of inhibitor which causes 50 per cent inhibition (I<sub>50</sub>) of an enzymatic reaction, *Biochem. Pharmacol.* 22 (1973) 3099–3108.
- [62] A. De Lean, P.J. Munson, D. Rodbard, Simultaneous analysis of families of sigmoidal curves: application to bioassay, radioligand assay, and physiological dose-response curves, *Am. J. Physiol.* 235 (1978) E97–E102.
- [63] G.C. González-Muñoz, M.P. Arce, B. López, C. Pérez, A. Romero, L. del Barrio, M.D. Martín-de-Saavedra, J. Egea, R. León, M. Villarroya, M.G. López, A.G. García, S. Conde, M.I. Rodríguez-Franco, N-acylaminophenothiazines: neuroprotective agents displaying multifunctional activities for a potential treatment of Alzheimer's disease, *Eur. J. Med. Chem.* 46 (2011) 2224–2235.
- [64] S. Hunskaar, O.B. Fasmer, K. Hole, Formalin test in mice, a useful technique for evaluating mild analgesics, *J. Neurosci. Methods.* 14 (1985) 69–76.
- [65] MOE: Chemical Computing Group Inc. Montreal. H3A2R7 Canada. <http://www.chemcomp.com>.
- [66] V. Cherezov, D.M. Rosenbaum, M.A. Hanson, S.G. Rasmussen, F.S. Thian, T.S. Kobilka, H.J. Choi, P. Kuhn, W.I. Weis, B.K. Kobilka, R.C. Stevens, High-resolution crystal structure of an engineered human beta<sub>2</sub>-adrenergic G protein-coupled receptor, *Science* 318 (2007) 1258–1265.
- [67] A. Bairoch, R. Apweiler, The SWISS-PROT protein sequence database and its supplement TrEMBL in 2000, *Nucleic Acids Res.* 28 (2000) 45–48.
- [68] H.M. Berman, J. Westbrook, Z. Feng, G. Gilliland, T.N. Beth, H. Weissig, I.N. Shindyalov, P.E. Bourne, The protein data bank, *Nucleic Acids Res.* 28 (2000) 235–242.
- [69] M. Levitt, Accurate modeling of protein conformation by automatic segment matching, *J. Mol. Biol.* 226 (1992) 507–533.
- [70] T. Fichteler, U. Dengler, D. Schomberg, Prediction of protein three-dimensional structures in insertion and deletion regions: a procedure for searching data bases of representative protein fragments using geometric scoring criteria, *J. Mol. Biol.* 253 (1995) 114–131.
- [71] W.D.C.P. Cornell, C.I. Bayly, I.R. Gould, K.M. Merz, D.M. Ferguson, D.C. Spellmeyer, T. Fox, J.W. Caldwell, P.A.J. Kollman, A second generation force field for the simulation of proteins, nucleic acids and organic molecules, *J. Am. Chem. Soc.* 117 (1995) 5179–5196.
- [72] C.D. Strader, M.R. Candelore, W.S. Hill, R.A. Dixon, I.S. Sigal, A single amino acid substitution in the beta-adrenergic receptor promotes partial agonist activity from antagonists, *J. Biol. Chem.* 264 (1989) 16470–16477.
- [73] G. Liapakis, J.A. Ballesteros, S. Papachristou, W.C. Chan, X. Chen, J.A. Javitch, The Forgotten Serine. A critical role for Ser-203<sup>5,42</sup> in ligand binding to and activation of the  $\beta$ 2-adrenergic receptor, *J. Biol. Chem.* 275 (2000) 37779–37788.
- [74] X.M. Guan, S.J. Peroutka, B.K. Kobilka, Identification of a single amino acid residue responsible for the binding of a class of beta-adrenergic receptor antagonists to 5-hydroxytryptamine1A receptors, *Mol. Pharmacol.* 41 (1992) 695–698.
- [75] Sybyl X 1.0, Tripos Inc, South Hanley Road, St Louis, Missouri, 1699, 63144, USA 25.